A Multi-Scale Model for the Intraseasonal Impact of the Diurnal Cycle over the Maritime Continent on the Madden-Julian Oscillation

Andrew J. Majda and Qiu Yang*

Department of Mathematics, and Center for Atmosphere-Ocean Science, Courant Institute, New York University, New York, New York

**Corresponding author address:* Qiu Yang, Courant Institute, New York University, 251 Mercer Street, New York, NY 10012

E-mail: yangq@cims.nyu.edu

ABSTRACT

The eastward propagating Madden-Julian Oscillation (MJO) typically exhibits complex behavior during its passage over the Maritime Continent, sometimes slowly propagating eastward and other times stalling and even terminating there with large amounts of rainfall. This is a huge challenge for present-day numerical models to simulate. One possible reason is the inadequate treatment of the diurnal cycle and its scale interaction with the MJO. Here these two components are incorporated into a simple self-consistent multi-scale model, which includes a model for the intraseasonal impact of the diurnal cycle and another one for the planetary/intraseasonal circulation. The latter model is forced self-consistently by eddy flux divergences of momentum and temperature from a model for the diurnal cycle with two baroclinic modes, which capture the intraseasonal impact of the diurnal cycle. The MJO is modelled as the planetary-scale circulation response to a moving heat source on the synoptic and planetary scales. The results show that the intraseasonal impact of the diurnal cycle during boreal winter tends to strengthen the westerlies (easterlies) at the lower (upper) troposphere in agreement with the observations. In addition, the temperature anomaly induced by the intraseasonal impact of the diurnal cycle can cancel that from the symmetric/asymmetric MJO with convective momentum transfer, yielding stalled or suppressed propagation of the MJO across the Maritime Continent. The simple multi-scale model should be useful for the MJO in observations or more complex numerical models.

1. Introduction

The Maritime Continent is a region in the tropical warm pool, consisting of islands, peninsulas and shallow seas. Due to strong insolation near the equator and low heat capacity of the land surface, tropical convection prevails over the Maritime Continent and releases a huge amount of latent heat to the atmosphere. Thus the Maritime Continent is considered as an important energy source region for the global circulation (Ramage 1968; Neale and Slingo 2003). Tropical convection over the Maritime Continent is organized on multiple time scales, ranging from cumulus clouds on the daily time scale to intraseasonal oscillations. In particular, on the daily time scale, the diurnal cycle of tropical convection over the Maritime Continent is very significant compared with that over the Indian Ocean and the western Pacific Ocean (Hendon and Woodberry 1993; Kikuchi and Wang 2008). On the intraseasonal time scale, the Madden-Julian Oscillation (MJO), the dominant component of the intraseasonal variability in the tropics, typically propagates eastward slowly across the Maritime Continent and can stall or terminate there along with large amounts of rainfall (Zhang 2005).

However, the contemporary general circulation models (GCMs) still do a poor job of resolving tropical convection over the Maritime Continent. One of the significant errors is that the GCMs cannot correctly simulate the precipitation over the Maritime Continent. For instance, obvious discrepancies of the diurnal amplitude in precipitation over the islands of the Maritime Continent during boreal winter have been noticed in the present-day GCM (Yang and Slingo 2001). Another one of the significant errors is that the GCMs typically poorly represent the eastward propagating MJO over the Maritime Continent (Inness and Slingo 2003; Sperber et al. 1997). One possible reason is the inadequate treatment of the diurnal cycle and its impact on the intraseasonal variability of atmospheric flow. In fact, current numerical models have difficulty in reproducing the diurnal variability of tropical precipitation (Dai and Trenberth 2004; Randall and Dazlich 1991; Tian et al. 2004), although superparameterization has enhanced fidelity (Benedict and Randall 2011; Khairoutdinov et al. 2005). In order to improve comprehensive numerical simulations with more realistic features, it is important to have a better understanding of the intraseasonal impact of the diurnal cycle and check whether such upscale impact from the diurnal cycle can influence the MJO.

In fact, many observational studies focus on the scale interaction between the diurnal cycle of precipitation and the MJO over the Maritime Continent (Peatman et al. 2014; Rauniyar and Walsh 2011; Chen and Houze 1997; Slingo et al. 2003). Among the previous studies, the modulation of the diurnal cycle of tropical convection by the MJO has been investigated by evaluating difference of the magnitude and phases of the diurnal cycle between the convectively active and suppressed phases of the MJO (Tian et al. 2006; Sui et al. 1997; Sui and Lau 1992). However, the upscale impact of the diurnal cycle of tropical convection on the MJO is not well understood. In the theoretical direction, the resonant nonlinear interactions between equatorial waves in the barotropic mode and the first baroclinic mode have been studied in the presence of a diurnally varying heat source, but the effect of the second baroclinic mode is not considered there (Raupp and Silva Dias 2009, 2010). In contrast to that, the multicloud models based on the first and second baroclinic modes for the three type clouds (congestus, deep and stratiform) have been built (Khouider and Majda 2006c,a,b, 2007, 2008b,a) and reproduce several realistic features of the diurnal cycle of tropical convection (Frenkel et al. 2011a,c, 2013).

The goal of this paper is to provide a framework for modelling the passage of the MJO over the Maritime Continent where the diurnal cycle of tropical convection is significant and assess how the intraseasonal impact of the diurnal cycle of tropical convection will modify the kinematic and thermodynamic characteristics of the MJO. Indeed, a self-consistent multi-scale model with two time scales (the daily/intraseasonal time scales) has been built to assess the intraseasonal impact of the diurnal cycle of tropical convection (Yang and Majda 2014). This multi-scale model provides two sets of equations governing planetary-scale tropical flow on the daily and intraseasonal time scales separately. It turns out that the planetary-scale circulation response on the intraseasonal time scale is forced by the eddy flux divergences of zonal momentum and temperature from the daily time scale. These eddy flux divergence terms provide us with assessment of upscale transfer of kinetic and thermal energy across multiple time scales in a transparent fashion.

According to this multi-scale model (Yang and Majda 2014), the planetary-scale tropical flow on the daily time scale is governed by a set of linear equations, which can be thermally forced by a heat source. Here we prescribe a diurnally varying heat source within a standing convective envelope to mimic the latent heat release over the Maritime Continent. In detail, we utilize the vertical structure in the first and second baroclinic modes for the heat source to characterize the diurnal cycle (Frenkel et al. 2011a,c, 2013) and the organized tropical convection with three type clouds (congestus, deep and stratiform) life cycle, which was first introduced in the multicloud models (Khouider and Majda 2006c,a,b, 2007, 2008b,a).

The planetary-scale tropical flow on the intraseasonal time scale is governed by another set of Gill-type equations in long wave approximation (Gill 1980; Matsuno 1966), which can be forced by the spatially upscale transfer from the synoptic scale to the planetary scale and the temporally upscale transfer from the daily time scale to the intraseasonal time scale as well as a mean heat source. In fact, the upscale transfer from the synoptic scale to the planetary scale from wave trains of thermally driven equatorial synoptic-scale circulations in a moving convective envelope and the direct mean heating have been studied previously in a multi-scale model for the MJO (Majda and Biello 2004; Biello and Majda 2005, 2006). In the similar model setup here, we consider three different scenarios of the MJO induced by synoptic-scale heating and planetary-scale heating, and all of them show some key features of the MJO such as the horizontal quadrupole structure and upward/westward tilted vertical structure. Then, by considering the upscale impact of the diurnal cycle from the daily time scale to the intraseasonal time scale, we are able to obtain the planetary-scale circulation response during the passage of the MJO over the Maritime Continent where the diurnal cycle of tropical convection is typically significant. The resulting flow field and temperature anomalies resemble some realistic features of the MJO behavior over the Maritime Continent including stalling or termination.

The rest of this paper is organized as follows. The model for the diurnal cycle and its upscale fluxes over the Maritime Continent are summarized in section 2. The planetary-scale circulation response to the intraseasonal impact of the diurnal cycle is shown in section 3. Section 4 describes three different scenarios for the MJO induced by synoptic-scale heating and planetary-scale heating. In section 5, we discuss the intraseasonal impact of the diurnal cycle on the MJO over the Maritime Continent and compare the resulting flow fields and temperature anomalies with the observations. The paper ends with concluding summary and discussion. The detailed description for the notation, dimensional units, parameters in the moving heat source for the MJO and the synoptic-scale equatorial weak temperature gradient equations (Majda and Biello 2004; Biello and Majda 2005, 2006) can be found in the appendix.

2. A model for the diurnal cycle and its upscale fluxes over the Maritime Continent

The diurnal variability of tropical convection has attracted attention in the scientific community in a long history. Early investigations of the diurnal variability of tropical precipitation can date back to the 1920s (Ray 1928). Due to the development of satellite measurements and computers, more global datasets in higher resolutions such as the Tropical Rainfall Measuring Mission (TRMM) are available for the community to study tropical convection in the tropics. In fact, the TRMM dataset has already been utilized to study the diurnal variations of the global tropical precipitation over land and oceans (Kikuchi and Wang 2008). By applying empirical orthogonal function (EOF) analysis to two complementary TRMM datasets (3B42 and 3G68) for 1998-2006, they concluded the persistence of the diurnal cycle of tropical precipitation with strong amplitude in the continental regime and weak amplitude in the oceanic regime. According to the figure 2 in the paper (Kikuchi and Wang 2008), the diurnal cycle of tropical convection over the Maritime Continent is more significant than that over the Indian Ocean and the western Pacific Ocean during boreal winter.

In the theoretical direction, the significant diurnal variability of tropical precipitation is examined in some simple models for tropical convection by considering three type clouds (congestus, deep and stratiform) to characterize organized tropical convection. (Frenkel et al. 2011b,d, 2013). Since the latent heat released in tropical convection can drive the tropical flow through thermodynamics, the diurnal cycle of tropical precipitation can induce the diurnal variability of the flow field. By following this underlying physical mechanism, the multi-scale model (Yang and Majda 2014) provides a set of equations governing the tropical flow associated with the diurnal cycle. In this section, we use this set of equations for the diurnal cycle and discuss the corresponding upscale fluxes on the planetary/intraseasonal time scale. The equations in non-dimensional units appropriate for the daily time scale read as follows,

$$\tilde{u}_t - y\tilde{v} = 0 \tag{1a}$$

$$\tilde{v}_t + y\tilde{u} = -\tilde{p}_y \tag{1b}$$

$$\tilde{\theta}_t + \tilde{w} = \tilde{S}_\theta \tag{1c}$$

$$\tilde{p}_z = \tilde{\theta} \tag{1d}$$

$$\tilde{v}_y + \tilde{w}_z = 0 \tag{1e}$$

where all physical variables such as the velocity $\tilde{u}, \tilde{v}, \tilde{w}$ and potential temperature $\tilde{\theta}$ have zero mean on the daily time scale. More details about the notation and the dimensional units can be found at Appendix A and the papers (Majda 2007; Yang and Majda 2014). Here we assume rigid-lid boundary conditions at top and bottom of the troposphere, $\tilde{w}|_{z=0,\pi} = 0$ where $z = 0, \pi$ represent the surface and top of the troposphere separately.

The large-scale tropical flow can be modelled as the atmospheric circulation response to diabatic heating (Gill 1980). Here the thermal forcing $\tilde{S}_\theta$ on the right side of Eq.1c is used to represent the latent heat release during tropical precipitation, thus a good cloud model can help to provide an appropriate heating profile. On the other hand, the multicloud model convective parameterizations (Khouider and Majda 2006c,a,b, 2007, 2008b,a) based on three cloud types (congestus, deep and stratiform) have successfully reproduced some crucial features of organized convection and tropical precipitation. In the multicloud models, the three types of clouds are highlighted and they serve to provide the bulk of tropical precipitation and the main source of latent heat in the troposphere. In detail, the cumulus congestus clouds heat the lower troposphere by latent heat release and cool the upper troposphere due to the detrainment and high reflectivity of the clouds top. The deep convective clouds can warm the whole troposphere along with the majority of tropical precipitation. The stratiform clouds can heat the upper troposphere through precipitation and cool the bottom due to the evaporation of rainfall. Therefore, the heating and cooling effects associated with these three clouds types exhibit the first and second baroclinic modes of vertical structure and here we incorporate these two baroclinic modes into the heating profile in dimensionless units to mimic diurnal variability (Frenkel et al. 2011a,c, 2013) as follows,

$$\tilde{S}_\theta = F(X) H(y) \left[\sin(kX + \omega t)\sin(z) + \alpha \sin(kX + \omega t + \beta)\sin(2z)\right] \tag{2}$$

$$F(X) = A_0 \cos\left[\frac{\pi X}{2L}\right]^+ ; H(y) = H_0 e^{-a(y-y_0)^2}. \tag{3}$$

Here $F(X)$ is the large-scale convective envelope function, which only depends on the planetary scale X in the zonal direction, while $H(y)$ is the meridional profile of the heat source. At each location with specific longitude and latitude, we utilize the first baroclinic mode for deep convective heating and the second baroclinic mode for congestus and stratiform heating. Both these two baroclinic modes are harmonically oscillating to mimic the diurnal cycle. The phase shift between these two modes β and the relative strength of the second baroclinic mode to the first baroclinic mode α are key parameters here. The exact expressions for the envelope function and parameter values can be found in Appendix B.

According to a main conclusion in (Yang and Majda 2014), the diurnal cycle of tropical convection has significant intraseasonal impact through eddy flux divergence of potential temperature associated with Eqs.1a-1e only during the solstices (boreal summer/boreal winter). Meanwhile, the eastward propagating MJO typically occurs during boreal winter. Therefore, we mainly focus on the case during boreal winter by setting the heating center of the envelope function south of the equator. Fig.1 shows the envelope function of the diurnal heating in longitude-latitude diagram during boreal winter, that is, $F(X)H(y)$ in Eq.2. This envelope function reaches maximum value at 1200 km south of the equator with about 6600 km width in zonal direction, which resembles the observation such as the figure 2(c) in (Kikuchi and Wang 2008). This envelope profile mimics the localized effect of the Maritime Continent in the model here.

Fig.2 shows the diurnal heating in time-height diagram for a given place with specific X, y, that is, $\sin(kX+\omega t)\sin(z)+\alpha\sin(kX+\omega t+\beta)\sin(2z)$. The alternating heating and cooling at a given height is due to the opposite thermal effects by congestus clouds and stratiform clouds as well as the intensification and diminishment of the deep convective clouds. In particular, the upward movement of the heating center can be used to describe the three clouds type (congestus, deep and stratiform) life cycle as well as mimicking key features of the diurnal cycle (Frenkel et al. 2011a,c, 2013).

Based on several essential assumptions and systematic multi-scale asymptotics, the multi-scale model (Yang and Majda 2014) shows that the resulting flow field forced by the diurnal heating model can generate eddy flux divergences of zonal momentum and temperature on the intraseasonal time scale,

$$F^u = -\frac{\partial}{\partial y}\langle \tilde{v}\tilde{u}\rangle - \frac{\partial}{\partial z}\langle \tilde{w}\tilde{u}\rangle\,; F^\theta = -\frac{\partial}{\partial y}\left\langle \tilde{v}\tilde{\theta}\right\rangle - \frac{\partial}{\partial z}\left\langle \tilde{w}\tilde{\theta}\right\rangle \tag{4}$$

which can further drive the planetary-scale circulation response on the intraseasonal time scale.

It has been shown in the appendix of (Yang and Majda 2014) that the existence of the second baroclinic mode for congestus/stratiform heating α and its phase shift from the first baroclinic mode β are essential for the intraseasonal impact of the diurnal cycle, which highlights the importance of the congestus and stratiform cloud heating during tropical convection for the large-scale tropical circulation, besides deep convection. However, the exact eddy flux divergences of zonal momentum and temperature are less sensitive to these two parameters α, β in the sense that their magnitudes are determined by the product $\alpha\sin(\beta)$ while their spatial patterns are independent of α and β. Fig.3 shows the eddy flux divergences of momentum and temperature in the latitude-height diagram during boreal winter. According to this figure, the dimensionless eddy flux divergences of zonal momentum from the diurnal cycle is weak and the eddy flux divergence of temperature provides dominating intraseasonal impact on the planetary-scale circulation. There is a significant heating center in the middle troposphere of the southern hemisphere and cooling surrounding this heating center. In addition, the magnitude of the heating in the middle troposphere is about two times as large as that of the cooling in upper and lower troposphere, which indicates that the first and third baroclinic modes are both significant in the intraseasonal impact of the diurnal cycle.

3. The planetary-scale circulation response to the intraseasonal impact of the diurnal cycle

The planetary-scale tropical flow can be modelled by the large-scale circulation response to a heat source such as the latent heat release during tropical precipitation (Gill 1980; Sobel et al. 2001). In these studies, the long wave approximation and weak temperature gradient approximation are discussed to further simplify the models. According to the multi-scale model (Majda 2007; Yang and Majda 2014), it turns out that the governing equations for the planetary-scale circulation response on the intraseasonal time scale is similar to the Gill-type model but also forced by upscale flux divergences of momentum and temperature from the daily time scale to the intraseasonal time scale. Due to the essential scaling assumptions for large-scale tropical flow, this set of equations is also in long wave approximation (Majda and Klein 2003; Majda and Biello 2004) and thus the eastward flow is in geostrophic balance with the pressure gradient. Furthermore, the zonal momentum damping and the radiative cooling have dissipation on the intraseasonal time scale (Lin et al. 2005; Romps 2014; Mapes and Houze Jr 1995) and therefore they can play a role here. The equations in dimensionless units read as follows,

$$U_T - yV = -P_X - dU + F^u \tag{5a}$$

$$yU = -P_y \tag{5b}$$

$$\Theta_T + W = -d_\theta \Theta + F^\theta \tag{5c}$$

$$P_z = \Theta \tag{5d}$$

$$U_X + V_y + W_z = 0 \tag{5e}$$

here all physical variables represent daily time scale mean and depend on the intraseasonal time scale T. The meridional circulation (V,W) is the secondary flow compared with that on the daily time scale. More details about the notation and the dimensional units can be found at Appendix A and the paper (Yang and Majda 2014). Here we assume rigid-lid boundary conditions at top and bottom of the troposphere, $W|_{z=0,\pi}=0$ where $z=0,\pi$ represent the surface and top of the troposphere separately. On the right side of Eqs.5a-5c, F^u, F^θ represent the eddy flux divergences of zonal momentum and temperature from the daily time scale to the intraseasonal time scale respectively,

$$F^u=-\frac{\partial}{\partial y}\langle\tilde{v}\tilde{u}\rangle-\frac{\partial}{\partial z}\langle\tilde{w}\tilde{u}\rangle;F^\theta=-\frac{\partial}{\partial y}\left\langle\tilde{v}\tilde{\theta}\right\rangle-\frac{\partial}{\partial z}\left\langle\tilde{w}\tilde{\theta}\right\rangle \tag{6}$$

here all these daily fluctuation components $\tilde{u}$, $\tilde{v}$, $\tilde{w}$, $\tilde{\theta}$ are from the model for the diurnal cycle in Sec.2.

Since the forcing terms F^u, F^θ only involve the daily fluctuation components $(\tilde{u},\tilde{v},\tilde{w},\tilde{\theta})$, the planetary-scale circulation is driven by the upscale feedback from the daily time scale to the intraseasonal time scale, as shown in the zonal momentum equation (Eq.5a) and the thermal equation (Eq.5c). By plugging such eddy flux divergences of zonal momentum and temperature shown in Fig.3 into Eqs.5a-5e, we are able to obtain the resulting planetary-scale circulation response with pressure perturbation and potential temperature anomaly. Fig.4 shows the horizontal flow field and pressure anomaly due to the intraseasonal impact of the diurnal cycle at upper troposphere ($z=11km$) and lower troposphere ($z=5km$). The main feature is that there is a cyclone (anti-cyclone) at the lower (upper) troposphere along with negative (positive) pressure perturbation in the southern hemisphere. The minimum (maximum) pressure perturbation in the lower (upper) troposphere is located south of the equator and slightly west of the diurnal heating center (the diurnal heating center is at $X=0$ shown in Fig.1). Such longitude difference between the pressure perturbation and diurnal heating can be explained by the westward propagating Rossby waves off the equator.

In addition, the thermodynamic characteristics of the planetary-scale circulation response on the intraseasonal time scale are crucial properties since they are related with cloudiness and precipitation in tropical convection. Fig.5 shows the temperature anomaly at the latitude-height diagram due to the intraseasonal impact of the diurnal cycle during boreal winter. The main feature is that in the southern hemisphere, there is a positive temperature anomaly in the middle troposphere and negative temperature anomaly in the upper and lower troposphere. The comparable magnitudes of positive and negative temperature anomalies at different heights indicate that the third baroclinic mode is quite significant here. Also, such a temperature anomaly even extends to the northern hemisphere but in much weaker magnitude. In a moist environment, negative potential temperature anomalies in the lower troposphere can increase the convective available potential energy(CAPE) and reduce the convective inhibition(CIN), which enhances the buoyancy of parcels in the free troposphere and provides a favorable condition for tropical convection. Meanwhile, the negative temperature anomaly reduces the saturation value of water vapor and promotes more convection in the lower troposphere. In contrast to that, the positive temperature anomaly in the middle troposphere can suppresses deep convection in the opposite way.

As a simple application, the Hadley cell can also be incorporated into this framework and is modified by the intraseasonal impact of the diurnal cycle of tropical convection (Yang and Majda 2014). The mean meridional circulation in the Hadley cell, which will advect the planetary-scale circulation response, can be derived by prescribing physically consistent momentum drag and heating. In an ideally zonally symmetric case, the resulting overturning motion induced by the intraseasonal impact of the diurnal cycle during boreal summer can strengthen the upper branch of the winter cell of the Hadley circulation but weaken the lower branch of the winter cell.

4. The MJO models forced by a moving heat source

On the intraseasonal time scale ($30-90$ days), the eastward propagating MJO is the most significant large-scale phenomenon in the tropical atmosphere, which typically initializes over the equatorial Africa, intensifies over the Indian Ocean, gets weakened over the Maritime Continent, sometimes redevelops over the western Pacific and dissipates near the date line (Rui and Wang 1990; Zhang 2005). The MJO is organized on multiple spatial scales and consists of coupled patterns of the wind field and tropical convection.

Although individual MJO events may vary in the magnitude of convection and the spatial patterns of atmospheric circulation in reality, the majority of the MJO events share several key features in the kinematic and thermodynamic characteristics, which should become important criterion for model validation. First of all, the velocity field exhibits horizontal quadrupole structure with flow convergence in the lower troposphere and divergence in the upper troposphere (Hendon and Salby 1994). At the lower troposphere, the easterly winds near the equator are accompanied by anticyclones to the east of the convection center. The westerly winds near the equator are accompanied by cyclones to the west of the convection center. At the upper troposphere, the horizontal quadrupole structure has opposite signs for wind directions and pressure perturbation. Secondly, the westerly wind burst has a distinct upward/westward tilt, meaning that the onset region of the westerly winds is located to the west compared with that at the surface (Lin and Johnson 1996; Yanai et al. 2000).

In the theoretical direction, several mechanisms have been proposed to improve our understanding of the MJO and a lot of numerical modelling has been done to capture the primary observed features of MJO (Zhang 2005). Having noticed that the planetary-scale circulation associated with the MJO also lives on the intraseasonal time scale, we can use the same equations Eqs.5a-5e from Sec.3 to model the MJO in a eastward propagating convective envelope. In fact, besides the upscale flux divergences of zonal momentum and temperature from the daily time scale, these equations in the full multi-scale model (Yang and Majda 2014) are also forced by the upscale flux divergence of zonal momentum and temperature from the synoptic scale (Majda and Biello 2004; Biello and Majda 2005). The latter has been interpreted as upscale transfer from synoptic to planetary scales of momentum and temperature and used to construct a multi-scale model for the MJO (Biello and Majda 2005). Here we build three such MJO models with different scenarios forced by the planetary-scale mean heating and the synoptic-scale heating in a moving convective envelope that exhibit several key features of the MJO as mentioned above.

a. the symmetric MJO with horizontal quadrupole structure induced by the planetary-scale heating

Although the individual MJO events may behave differently from each other, the statistical composites of reanalysis data provides insight into the horizontal structure of the MJO envelope with key features (Hendon and Salby 1994). One of the significant features of the MJO is its horizontal quadrupole structure with cyclone/anticyclone pairs in both the lower troposphere and upper troposphere. In detail, at the lower troposphere, there are easterlies east of the convection coupling with two anticyclones and westerlies coupling with two cyclones on both subtropics. At the upper troposphere, there are westerlies east of the convection coupling with two cyclones and easterlies coupling with twin anticyclones on both subtropics.

In a long period with multiple MJO events, the overall convection field intensifies and diminishes with changing rainfall at each specific location, which corresponds to the alternating active and suppressed phases of the MJO. Here we prescribe the planetary-scale heating for latent heat release during tropical convection as follows

$$\left\langle S^{\theta} \right\rangle = F\left(X - st\right) H\left(y\right) \left[\sin\left(z\right) + \alpha \sin\left(2z\right)\right] \tag{7}$$

$$F(X) = A_0(a^2 - X^2)e^{-a_0 X^2}; H(y) = H_0 e^{-(y-y_0)^2} \tag{8}$$

the envelope function $F\left(X - st\right))$ is used to mimic the eastward moving convective envelope and in Eq.7 and below, the MJO phase speed is prescribed by $s = 5ms^{-1}$. Different from the standard mean heating used by (Biello and Majda 2005), the envelope function $F(X)$ used here is positive in the middle and negative on both sides, which resembles the active phase of the MJO in the middle and suppressed phases on the two sides. In fact, such an envelope function is crucial for the quadrupole structure of the resulting circulation response. The meridional profile $H(y)$ is a Gaussian shape function, symmetric about the equator. The relative strength of the second baroclinic mode $\alpha = -0.25$ is a parameter to adjust the heating center in height. The exact expressions for the heating profile and parameter values can be found in Appendix B.

As for the vertical structure of the heating in Eq.7, the first baroclinic mode represents deep convection with maximum latent heat release in the middle troposphere. The second baroclinic mode with negative strength coefficient α can be interpreted as stratiform precipitation with latent heat in the upper troposphere and cooling in the lower troposphere due to rain evaporation. The combination of these two baroclinic modes leads to the top-heavy heating profile as shown in (Kiladis et al. 2005). Fig.6 shows the longitude-height diagram for the planetary-scale heating at the equator. There is top-heavy heating in the middle of the convection envelope and cooling to the east and west of the convection region. The planetary-scale heating decays as the latitude increases.

After prescribing such planetary-scale heating as shown in Fig.6, we can obtain the planetary-scale circulation response on the intraseasonal time scale by letting this heating to thermally force the Eqs.5a-5e. Fig.7 shows the horizontal flow fields with pressure perturbation at the lower troposphere ($z = 5$km) and upper troposphere ($z = 11km$). The horizontal quadrupole structure is clear at both levels. In addition, the pressure anomalies are quite weak in the sense that its magnitude is much less than 1 in dimensionless units. Meanwhile, the zonal winds at the lower and upper troposphere are out of phase, which is consistent with the low-level flow convergence and upper-level flow divergence.

b. the symmetric MJO with westerly winds burst induced by synoptic-scale heating and planetary-scale heating

A multi-scale model for the MJO with two spatial scales (the synoptic scale and planetary scale) has been developed by (Majda and Biello 2004; Biello and Majda 2005, 2006). This model accounts for both the upscale transfer from the synoptic scale to the planetary scale of momentum and temperature from wave trains of thermally driven equatorial synoptic-scale circulations in a moving convective envelope as well as direct mean heating on the planetary scale. In addition, the model prescribes the heat source with dominant low-level congestus convection to the east of the moving convective envelope and dominant upper-level supercluster activity to the west.

Here we construct the two-scale MJO model driven by both the synoptic-scale heating and planetary-scale heating in a similar way. The planetary-scale mean heating is similar to that in Eq.7 but with $\alpha = 0$ and $A_0 = 44.8$ in Eq.7-8, which is used to mimic deep convection at the alternating active and suppressed phases of MJO on the planetary scale. On the synoptic scale, there are equatorial synoptic-scale heating in a eastward moving planetary-scale convective envelope.

The synoptic-scale heating, in dimensionless units, reads as follows,

$$S_\theta' = F\left(X - sT\right) H\left(y\right) \left\{ \cos\left(\frac{x}{\lambda} - \phi\left(T\right)\right) \sin\left(z\right) - \alpha\left(X - sT\right) \cos\left(\frac{x + x_0}{\lambda} - \phi\left(T\right)\right) \sin\left(2z\right) \right\} \tag{9}$$

$$F(X - sT) = A_0 \cos\left[\frac{\pi(X - sT)}{2L_F}\right]^+ ; H(y) = H_0 e^{-a_0(y - y_0)^2} ; \alpha\left(X - sT\right) = -\frac{8\left(X - st\right)}{3L_F} \tag{10}$$

here $F(X - st)$ is the moving envelope function where $s = 0.1$ corresponds to $5ms^{-1}$. The magnitude of the convective envelope $A_0 = 1$ is chosen to yield realistic magnitudes of wind, etc. The meridional profile $H(y)$ is a Gaussian shape function, symmetric about the equator. The first and second baroclinic modes are modulated by wave trains on the synoptic scale. All the parameter values and their interpretation can be found in Appendix B and (Biello and Majda 2005).

Through the assumption that the synoptic-scale heating only depends on the intraseasonal time scale T instead of the daily time scale t, the synoptic-scale fluctuation components for all physical variables satisfy the synoptic-scale equatorial weak temperature gradient (SEWTG) equations (shown in Appendix C), which has been discussed in (Majda and Biello 2004; Biello and Majda 2005, 2006). In the SEWTG equations, both the momentum and thermal damping do not play a role because of their longer time scale. Fig.8 shows the contours of synoptic scale heating on the synoptic scale longitude-height diagram with the maximum heating and cooling in the upper troposphere, which resembles the diabatic heating observed in reality (Kiladis et al. 2005). The heating is upward/westward tilted with consistent rising and sinking motion, which is used to characterize organized convective superclusters in the convective envelope.

According to the full multi-scale model (Yang and Majda 2014), the planetary-scale circulation response can also be forced by the spatially upscale transfer from the synoptic scale to the planetary scale, besides the temporally upscale transfer from the daily time scale to the intraseasonal time scale. This spatially upscale transfer from the synoptic scale of zonal momentum and temperature can be expressed as follows,

$$F^u = -\overline{(u'v')}_y - \overline{(u'w')}_z; F^\theta = -\overline{(\theta'v')}_y - \overline{(\theta'w')}_z \tag{11}$$

here u', v', w', θ' are the fluctuation components with zero mean on the synoptic scales. The bar represents spatial averaging on the synoptic scale and its exact definition can be found at Appendix A.

Then we can consider the superimposition effect of the planetary-scale heating (Eq.7) and the upscale transfer from the synoptic scale of zonal momentum and temperature (Eqs.11), and let the combined forcing drives the planetary-scale circulation response on the intraseasonal time scale (Eqs.5a-5e). Here for clear display, we reduce the magnitude of the planetary-scale heating to $\frac{4}{5}$ of its original value. Fig.9 shows the horizontal flow field with pressure perturbation from this MJO model. The horizontal quadruple structure can be found clearly at the surface, the lower and upper troposphere. In addition, the horizontal flow field indicates flow convergence at the lower troposphere with upward/westward titled westerlies .

On the other hand, the potential temperature anomaly field is one of the crucial thermodynamic characteristics of the MJO. Fig.10 shows the horizontal flow field and temperature anomaly from the same MJO model above. One of the significant features is that there is very significant third baroclinic mode around the center of the convective envelope, which is intuitively consistent with the hydrostatic balance assumption. The magnitude of cold temperature anomaly at the middle troposphere is larger than those of warm temperature anomaly at both the upper and lower troposphere, which also indicates the significance of the first baroclinic mode for the deep convection.

c. the asymmetric MJO with upward/westward tilt induced by synoptic-scale heating and planetary-scale heating

Some MJO observation indicates that seasonal variations in convective activity can also affect the planetary-scale flow (Lin and Johnson 1996). On the other hand, the zonal winds and temperature anomalies associated with the MJO exhibit upward/westward tilted vertical structure according to the observation (Lin and Johnson 1996; Kiladis et al. 2005). Therefore, it is interesting to construct a model for the MJO in tilted vertical structure of easterlies and temperature anomalies, which also propagates eastward off the equator, following (Biello and Majda 2005).

Here we consider a meridionally asymmetric MJO model forced by both the synoptic-scale heating and planetary-scale heating in a moving convective envelope off the equator. Meanwhile, the heating both on the synoptic and planetary scales are upward/westward tilted, which reflects the similarity of tropical convection across multiple scales. The synoptic-scale heating can be expressed by Eq.9 except that the maximum heating is located at 900 km south of the equator. In contrast to the planetary-scale heating with constant relative strength of the second baroclinic mode (Eq.7), here we vary the relative strength of the second baroclinic mode α so that the heating center is located at the lower troposphere to the east and the upper troposphere to the west. Such planetary-scale heating can be used to characterize the low-level congestus heating to the east of the convection envelope and upper troposphere supercluster heating to the west. The planetary-scale heating, in dimensionless units, reads as follows

$$\overline{S^{\theta}} = F(X-st)H(y)\left[\sin(z) + \frac{3(X-sT)}{2L_F}\sin(2z)\right] \tag{12}$$

$$F(X-sT) = A_0\cos\left[\frac{\pi(X-sT)}{2L_F}\right]^{+}; H(y) = H_0 e^{-(y-y_0)^2} \tag{13}$$

where the envelope function $F(X-st)$ is used to mimic the eastward moving convective envelope. Compared with the planetary-scale heating in Eq.7 with constant relative strength of the second baroclinic mode, the heating in Eq.12 has a relative strength coefficient in a linear function so that the vertical profiles of the heating are different within the convective envelope. The meridional profile $H(y)$ is a Gaussian shape function which is asymmetric about the equator. The exact expressions for the heating profile and parameter values can be found in Appendix B.

Similarly, we can consider the superimposition effect of the planetary-scale heating (Eq.12) and the upscale transfer from the synoptic scale of zonal momentum and temperature (Eqs.11) with the off-equator meridional profile, and let the combined forcing drives the planetary-scale circulation response on the intraseasonal time scale (Eqs.5a-5e). Fig.11 shows the horizontal flow field and pressure perturbation from the meridionally asymmetric MJO model with the synoptic-scale and planetary-scale heating centered at 900 km south. At the equator, there are flow convergence in the lower troposphere and flow divergence in the upper troposphere. The horizontal profiles of the pressure and flow field exhibit strong asymmetry with only one anticyclonic/cyclonic pair of gyres south of the equator.

Again, the potential temperature anomaly field is one of the crucial thermodynamic characteristics of the MJO. Fig.12 shows the horizontal flow field and temperature anomaly in the meridionally asymmetric MJO model with the synoptic-scale and planetary-scale heating at 900 km south. One of significant features is that the temperature anomalies exhibit significantly the first and third baroclinic modes with cold temperature anomaly in the middle troposphere and warm temperature anomaly in both the upper and lower troposphere.

5. The intraseasonal impact of the diurnal cycle over the Maritime Continent on the MJO

The MJO consists of large-scale dynamic field and tropical convection field in a coherent structure and typically propagates eastward from the Indian Ocean to the Maritime Continent to the western Pacific Ocean (Zhang 2005). Due to the complex topography and tropical convection over the Maritime Continent, the MJO exhibits quite different velocity and thermodynamic characteristics there than those over other regions (Wu and Hsu 2009). For example, the convection field associated with the MJO usually gets weakened during its passage over the Maritime Continent (Rui and Wang 1990). Furthermore, when the MJO is in the Indian Ocean, its convective center sits in the region with flow convergence at the surface. After the MJO goes across the Maritime Continent, the dynamic field has faster propagation speed than the convection field so that the upper-level easterlies and low-level westerlies include the convection center (Rui and Wang 1990).

As we already know the fact that the diurnal cycle of tropical convection is very significant over the Maritime Continent (Kikuchi and Wang 2008), one possible reason for the complex MJO behaviors is its scale interaction with the diurnal cycle of precipitation based on the observation evidence(Peatman et al. 2014). In the theoretical direction, based on the multi-scale model (Yang and Majda 2014), we conclude in Sec.2-3 that the diurnal cycle has significant impact on both the atmospheric circulation and the temperature anomalies during boreal winter. By adding the intraseasonal impact of the diurnal cycle during the passage of the MJO over the Maritime Continent, we can investigate how the intraseasonal impact of the diurnal cycle will modify the velocity and thermodynamic characteristics of the MJO and get intuition and mechanisms for the complicated behavior of the MJO. Since we have already built three different models with some key features of the MJO in Sec.4, in this section, we will discuss the intraseasonal impact of the diurnal cycle on these different MJOs separately.

a. the symmetric MJO with horizontal quadrupole structure induced by the planetary-scale heating

The relative phase between the surface winds and convection center varies during the eastward propagation of the MJO from the Indian Ocean to the western Pacific Ocean. When the MJO intensifies in the Indian Ocean, the convective center matches the surface flow convergence. During the passage of the MJO over the Maritime Continent, however, the westerlies dominates and thus the convection center is situated in low-level westerly winds, which is suggested by several observational studies. For example, Sui and Lau (1992) studied multiscale variability in the atmosphere during the boreal winter in 1979 and identified two intraseasonal oscillations (ISOs) within the equatorial belt. They found that persistent westerly winds are established in the region between 120° and 180° throughout the northern winter season. Such persistent westerly winds are also observed in the monsoon intraseasonal variability of 1987/1988 between 105° and 150° in the southern hemisphere (Waliser and Lau 2005). In addition, Rui and Wang (1990) investigated the development and dynamical structure of intraseasonal low-frequency convection anomalies in the equatorial region with 200 and 850 mb wind data and found that there are strong westerlies over the convection region when the convection anomaly reaches the Maritime continent.

If we assume that the eastward propagating MJO can keep the coupled structure of atmospheric circulation and convection as the one in the Indian Ocean, there are easterly winds to the east of the convection center and westerly winds to the west. However, as the observation shows, there are persistent westerly winds during the passage of the MJO over the Maritime Continent. The significant diurnal cycle over the Maritime Continent can be the essential reason. Due to the intraseasonal impact of the diurnal cycle of tropical convection, the resulting cyclone dominates in the lower troposphere of the southern hemisphere and generates westerlies at low latitudes of the southern hemisphere as shown in Fig.4, which can explain the persistent lower-level westerly winds over the Maritime Continent. If the strong westerlies due to the intraseasonal impact of the diurnal cycle can dominate over the Maritime Continent in the southern hemisphere, the resulting low-latitude westerlies can be significant during the passage of the MJO. Here we consider both the MJO with horizontal quadrupole structure (Sec.4a) and the intraseasonal impact of the diurnal cycle in Sec.3. Fig.13 shows the horizontal velocity field under the impact of both MJO and diurnal cycle at 5 km. The black box denotes the region between $15°S \sim 0°$ over the Maritime Continent where the diurnal cycle is significant during boreal winter. One crucial feature is that during the passage of the MJO, there are persistent westerly winds in the region denoted by the black box in Fig.13, which matches well with the observations mentioned earlier.

As for the upper troposphere, the convection center is situated in upper-level easterlies during the passage of the MJO across the Maritime Continent. Rui and Wang (1990) investigated the development and dynamical structure of intraseasonal low-frequency convection anomalies in the equatorial region with 200 and 850 mb wind data. They found that during the period when the MJO convection anomaly reaches the Maritime Continent, there are strong 200 mb easterlies over the Maritime Continent in the southern hemisphere. If we assume that the eastward propagating MJO can keep the coupled structure of atmospheric circulation and convection as the one in the Indian Ocean, there are westerly winds to the east of the convection center and easterly winds to the west at the upper troposphere, which does not match the observation described above. One of the reasons is the intraseasonal impact of the diurnal cycle. Due to the anticyclone in the upper troposphere of the southern hemisphere induced by the diurnal cycle (shown in Fig.4), the resulting upper-level easterlies at low latitudes of the southern hemisphere can explain the persistent upper-level easterly winds over the Maritime Continent. Here we consider both the MJO with horizontal quadrupole structure (Sec.4a) and the intraseasonal impact of the diurnal cycle in Sec.3. Fig.14

shows the horizontal velocity field under the impact of both MJO and diurnal cycle at 12 km. The white box denotes the region where the diurnal cycle is significant during boreal winter. There are strong easterly winds over the region denoted by the white box when the convection center moves to Maritime Continent, which matches the observations well.

In order to explore the primary structure of the vertical motion, Rui and Wang (1990) also calculate the differential divergence $D_{200} - D_{850}$, which can be considered as an estimate of the vertical motion at middle troposphere. One significant feature is that at the period when the convection center reaches the Maritime Continent, the large differential divergence anomaly also moves into the Maritime Continent and reaches its maximum magnitude at the low latitude of the southern hemisphere, meaning the intensifying rising motion in the middle troposphere. On the other hand, the intraseasonal impact of the diurnal cycle induce a heating center in the middle troposphere of southern hemisphere and cooling in the upper and lower troposphere (shown in Fig.3).Correspondingly, there is rising motion dominating in the middle troposphere of the southern hemisphere. Thus one possible reason for the intensifying rising motion in the middle troposphere is due to the diurnal cycle. Here we use the same model setup as above and Fig.15 shows the contour of vertical motion at the middle troposphere ($z = 7.85$ km) associated with both the MJO and the intraseasonal impact of diurnal cycle. The white box denotes the region where the diurnal cycle is significant during boreal winter. One significant feature in this figure is that when the MJO moves to the region denoted by the white box, the rising motion associated with the MJO is strengthened a lot due to the intraseasonal impact of diurnal cycle, which resembles the observation described above.

b. the symmetric MJO with westerly winds burst induced by synoptic-scale heating and planetary-scale heating

The individual MJO events usually differ to each other in the propagation extent and the convection strength. In order to guarantee the statistical significance, the composite MJO is often utilized to represent some key features of the MJO events based on a longer time period of observational data from satellites. By focusing on the composite MJO using 10 years of outgoing longwave radiation (OLR) and 7 years of wind data, Rui and Wang (1990) found that the eastward propagating convective anomaly typically gets weakened in the Maritime Continent (Rui and Wang 1990). One of the explanations for such weakening convection anomaly is attributed to the direct topographic effect such as blocking and wave-making effects (Wu and Hsu 2009). Alternatively, here we try to explain the weakening MJO convection by the intraseasonal impact of the diurnal cycle of tropical convection over the Maritime Continent, which can be interpreted as the indirect topographic effect since the significant diurnal cycle is associated with the low heat capacity of the land (Frenkel et al. 2011a,c, 2013).

Here we consider both the symmetric MJO with westerly winds burst in Sec.4b and the intraseasonal impact of the diurnal cycle in Sec.3. The relative strength of the diurnal cycle is adjusted to $\frac{3}{4}$ so that the magnitude of its temperature anomaly is comparable with that from the MJO. In order to fully discuss the intraseasonal impact of the diurnal cycle on the MJO, it is interesting to consider different phases of the MJO during its passage over the Maritime Continent. Here we use three phases (phase I, phase II, phase III) to denote different longitudes where the MJO convective center is located. Phase I corresponds to the case when the MJO convective center is 8.1×10^3 km to the west of the diurnal cycle heating center. In phase II, the MJO convective center is 2.4×10^3 km to the west and phase III is the case with the MJO convective center 3.2×10^3 km to the east.

Fig.16-18 show the total planetary-scale circulation response with temperature anomaly as the MJO propagates across the Maritime Continent. Meanwhile, the diurnal cycle of tropical convection is assumed to be significant over the Maritime Continent during boreal winter. The center of the diurnal cycle heating is set at $X = 0$. One important feature is that at Phase II, the temperature anomaly south of the equator associated with the MJO is weakened by the intraseasonal impact of the diurnal cycle. In fact, the intraseasonal impact of the diurnal cycle introduces a temperature anomaly in the first and third baroclinic modes, which is in opposite sign with that from the MJO model. Such temperature anomaly cancellation can potentially explain the fact that the MJO convection field gets weakened and even stalls during its passage over the Maritime Continent.

c. the asymmetric MJO with upward/westward tilt induced by synoptic-scale heating and planetary-scale heating

It is also interesting to consider the asymmetric MJO with upward/westward tilt when the MJO convective center located south of the equator. Here we consider both the symmetric MJO with westerly winds burst in Sec.4c and the intraseasonal impact of the diurnal cycle in Sec.3. The relative strength of the diurnal cycle is adjusted to its 0.8 so that the magnitude of its temperature anomaly is comparable with that from the MJO. Also, we consider the three phases (phase I, phase II, phase III) as Sec.5b. Fig.19-21 shows the temperature anomaly under the intraseasonal impact of the diurnal cycle during the passage of the asymmetric MJO at Phase I, II and III. During the phase II, the temperature anomaly in the active phase of the MJO is cancelled by that from the intraseasonal impact of the diurnal cycle. Such weakening temperature anomaly can potentially explain the fact that some MJOs gets weakened and even stalls during its passage over the Maritime Continent.

6. Concluding summary and discussion

Tropical convection over the Maritime Continent is organized on multiple spatiotemporal scales, ranging from cumulus clouds on the daily time scale over a few kilometers to intraseasonal oscillations over planetary scales. The diurnal cycle, the significant process on the daily time scale, has stronger magnitude over the Maritime Continent than that over the Indian Ocean and the western Pacific Ocean. On the other hand, the MJO, the significant component of the intraseasonal variability of tropical convection, typically propagates eastward across the Maritime Continent during boreal winter. To improve the present-day comprehensive numerical simulations for tropical convection over the Maritime Continent, a better understanding about the scale interaction between the diurnal cycle and the MJO is necessarily required. In this article, we focus on the intraseasonal impact of the diurnal cycle over the Maritime Continent on the MJO during boreal winter.

In the theoretical direction, the multi-scale analytic model with two time scales (daily/intraseasonal) provides assessment of the intraseasonal impact of planetary-scale inertial oscillations in the diurnal cycle (Yang and Majda 2014). In detail, this multi-scale model provides two sets of equations governing planetary-scale tropical flow on the daily and intraseasonal time scale separately. Here we use the set of equations on the daily time scale to model the diurnal cycle and that on the intraseasonal time scale for the planetary-scale circulation response on the intraseasonal time scale. The latter is forced by eddy flux divergences of zonal momentum and temperature from the daily time scale. Furthermore, the full multi-scale model considers two spatial scales (synoptic/planetary) and two time scales(daily/intraseasonal), and thus the planetary-scale circulation response is also forced by eddy flux divergences of zonal momentum and temperature from the synoptic scale to the planetary scale. In fact, the upscale transfer from the synoptic scale to the planetary scale of momentum and temperature has been applied to successfully model the MJO based on its multi-scale features (Majda and Biello 2004; Biello and Majda 2005, 2006).

In the model for the diurnal cycle, diurnal heating in the first and second baroclinic mode is prescribed to mimic latent heat release associated with three cloud types (congestus, deep and stratiform) life cycle (Frenkel et al. 2011a,c, 2013). Such organized tropical flow in the diurnal cycle can generate eddy flux divergences of momentum and temperature, which further drives the planetary-scale circulation response on the intraseasonal time scale (Yang and Majda 2014). In particular, here we consider the diurnal heating during boreal winter with the heating center sitting to the south of the equator. The resulting upscale flux divergence of temperature has the dominating impact on the circulation response and exhibits a heating center in the middle troposphere of the southern hemisphere and cooling at both the upper and lower troposphere surrounding the heating center. The corresponding planetary-scale circulation response on the intraseasonal time scale shows that such intraseasonal impact of the diurnal cycle can induce a cyclone (anticyclone) in the lower (upper) troposphere as well as significant temperature anomalies in the tropics. In a moist environment, particularly, the negative potential temperature anomaly in the lower troposphere can increase the convective available potential energy(CAPE) and reduce the convective inhibition(CIN), which enhances the buoyancy of parcels in the free troposphere and provides a favorable condition for tropical convection. Meanwhile, the negative temperature anomaly reduces the saturation value of water vapor and promotes more convection in the lower troposphere. A positive temperature anomaly in the middle troposphere has the opposite effect and can suppress deep convection.

By using the planetary-scale equations on the intraseasonal time scale, we model the original MJO by the circulation response in a moving heat source without the impact of the diurnal cycle. Since the real individual MJO events may differ in convection magnitude and circulation pattern to each other, we consider MJO models forced by three different types of the synoptic/planetary heating in a moving heat source. Each MJO model can capture several key features of the MJO such as the horizontal quadrupole structure and upward/westward tilt. Then, by considering the diurnal cycle during the passage of the MJO over the Maritime Continent, we try to answer the questions how the intraseasonal impact of the diurnal cycle will modify the behavior of the original MJO and whether the resulting kinematic and thermodynamic characteristics match the observations.

The results are as follows. For the MJO with the horizontal quadrupole structure induced by the planetary-scale heating, the intraseasonal impact of the diurnal cycle tends to strengthen westerly winds in the lower troposphere and easterly winds in the upper troposphere during the passage of the MJO over the Maritime Continent, which explains the fact that the MJO convection center typically sits in the westerlies in the lower troposphere and easterlies in the upper troposphere there. In addition, the intraseasonal impact of the diurnal cycle can also strengthen the vertical motion in the middle troposphere. As for the symmetric MJO with westerly wind burst induced by the synoptic-scale and planetary-scale heating, the temperature anomaly associated with the MJO tends to get cancelled by that from the intraseasonal impact of the diurnal cycle, which can explain the fact that MJO events typically get weakened across the Maritime Continent. In fact, such temperature anomaly cancellation is also significant in the asymmetric MJO with upward/westward tilt induced by the synoptic-scale and planetary-scale heating. Tung et al. (2014) found that during the passage of the MJO over the Maritime Continent, the symmetric MJO signals such as the heating and drying signals diminish entirely and the corresponding off-equatorial signals propagates with weakening strength. In contrast, the off-equatorial convection in the asymmetric MJO convection passes the Maritime Continent without inhibition. One possible factor developed here to support the asymmetric MJO propagating off the equator is the negative temperature anomaly induced by the intraseasonal impact of the diurnal cycle, which provides a favorable condition for tropical convection off the equator.

This study has several important implications for physical interpretation and model prediction. First, the diurnal cycle of tropical convection has significant upscale transfer of temperature from the daily time scale to the intraseasonal time scale through temperature flux divergence, which leads to another mechanism about the upscale impact of tropical convection from small spatiotemporal scales, besides convective momentum transport (Majda and Biello 2004; Biello and Majda 2005). Secondly, the intraseasonal impact of the diurnal cycle can significantly modify the MJO during its passage over the Maritime Continent, which helps to explain the complex behavior of the MJO over the Maritime Continent and its scale interaction with the diurnal cycle. Thirdly, it emphasizes the significance of the representation of the diurnal variability of tropical precipitation for comprehensive numerical simulations. The present model can also be elaborated in several ways. For example, the diurnal heating prescribed here is assumed to have zero mean on the daily time scale. The diurnal heating with nonzero daily mean can generalize the framework and may be more realistic for the tropical convection over the Maritime Continent. In addition, we only consider the diurnal cycle of tropical convection on the planetary scale here. The diurnal cycle on the synoptic scale or even smaller scales can be interesting for modelling individual tropical convection events such as cumulus clouds.

Acknowledgments. This research of A.J.M is partially supported by the office of NAVAL Research ONR MURI N00014-12-1-0912, and Q.Y. is supported as a graduate research assistant on this grant.

APPENDIX A

the dimensional units and notation in the multi-scale model

The full multi-scale model for the intraseasonal impact of the diurnal cycle of tropical convection (Yang and Majda 2014) is derived from the hydrostatic, anelastic Euler equations on an equatorial β-plane,which are the appropriate equations for large-scale phenomenon in the tropical troposphere. This derivation follows using multiple-scale techniques developed in (Majda and Klein 2003; Majda 2007). These equations have been nondimensionalized first so that time scale is measured in units of the equatorial time scale $T_E = (c\beta)^{-1/2} \approx 8.3h$, the horizontal length scale is in units of the equatorial deformation radius $L_E = (c/\beta)^{1/2} = 1500km$, the vertical length scale is in units of the troposphere height divided by π, $H = H_T/\pi \approx 5km$. Here c is defined as the dry Kelvin wave speed and β denotes the Rossby parameter in the Beta plane approximation. The free troposphere occupies the domain $-20*10^3km \le x \le 20*10^3km$, $-5*10^3km \le y \le 5*10^3km$, $0km \le z \le 16km$. The dimensional units for all physical variables and some constant parameters are summarized in Table 1.

In order to consider the large-scale quantities after averaging about the small scales, two averaging operators on the synoptic scale and daily time scale have been defined as follows

$$\bar{f}(X,t,T,y,z) = \lim_{L\to\infty} \frac{1}{2L} \int_{-L}^{L} f(x,X,t,T,y,z)\,dx \tag{A1}$$

$$\langle f \rangle (x,X,T,y,z) = \lim_{T^*\to\infty} \frac{1}{2T^*} \int_{-T^*}^{T^*} f(x,X,t,T,y,z)\,dt \tag{A2}$$

For all physical variables f, we can have its planetary-scale mean and synoptic-scale fluctuation decomposition $f = \bar{f} + f'$ and f' satisfies $\bar{f}' = 0$. Similarly, we can also have the intraseasonal time mean and daily fluctuation decomposition $f = \langle f \rangle + \tilde{f}$ and $\tilde{f}$ satisfies $\langle \tilde{f} \rangle = 0$.

By using the averaging operator on the daily time scale, we can define the daily time mean for all physical variables as follows, $U = \langle u \rangle$, $V = \langle v_2 \rangle$, $W = \langle w_2 \rangle$, $\Theta = \langle \theta \rangle$,$P = \langle u \rangle$. Here v_2 and w_2 are at the second order and u, p, θ are at the first order in the asymptotic expansion.

APPENDIX B

the expressions and parameters in the heating profile for the diurnal cycle and MJO

a. the heating profile for the diurnal cycle

In the heating profile for the diurnal cycle in Eq.2, the envelope function $F(X)$ and the meridional profile $H(y)$ are chosen as follows,

$$F\left(X\right) = A_0 \cos\left[\frac{\pi X}{2L}\right]^{+}; H\left(y\right) = H_0 e^{-a(y-y_0)^2} \tag{B1}$$

here $F(X)$ is chosen to be half cosine function to mimic the Maritime Continent in about $6600km$ longitude width ($L = \frac{2}{9}$), and its magnitude is $A_0 = \sqrt{5}$. The symbol for half cosine function used in the following context has the same meaning. The meridional profile is chosen to be a Gaussian shape function for simplicity. $y_0 = -0.8$ is chosen to mimic the case for boreal winter so that the latitude with maximum magnitude is at $10.8°S$, $H_0 = 1, a = 2$. The dimensionless parameters $\alpha = 2/3, \beta = \pi/4$ are chosen to be physically consistent with the three type clouds (congestus, deep and stratiform) life cycle. The dimensionless k is chosen to be wavenumber 1 and ω corresponds to 1 day frequency for the diurnal cycle.

b. the heating profile in the MJO model at the section 4a

In the MJO model in Eq.7, the envelope function of the heating $F(X)$ and the meridional profile $H(y)$ are chosen as follows,

$$F(X) = A_0(a^2 - X^2)e^{-a_0 X^2}; H(y) = H_0 e^{-(y-y_0)^2} \tag{B2}$$

here we choose the parameters in the envelope function $A_0 = 56$, $a = 0.2357$, $a_0 = 9$ so that the zonal average of $F(X)$ around the equator is zero. Such envelope function can mimic the planetary-scale convection with the active phase in the middle and suppressed phases on the two sides. Also, the circulation response to the planetary-scale heating is not sensitive to the damping coefficients due to the zero zonal mean. As for the meridional profile, we choose $H_0 = 2, y_0 = 0$ to mimic the MJO when it propagates along the equator and the convection is trapped around equatorial regions. In order to mimic the deep convection and stratiform clouds heating, we choose $\alpha = -\frac{1}{4}$.

c. the heating profile in the MJO model at the section 4b

In the MJO model in Eq.9, the envelope function of the heating $F(X - sT)$ and the meridional profile $H(y)$ are chosen as follows,

$$F(X - sT) = A_0 \cos\left[\frac{\pi (X - sT)}{2L_F}\right]^+ ; H(y) = H_0 e^{-a_0 (y - y_0)^2} ; \alpha (X - sT) = -\frac{8(X - st)}{3L_F} \qquad \text{(B3)}$$

here $L_F = 1/3$ represents 5000 km half width of the envelope, $A_0 = 1$. y_0 can be adjusted for different seasons, $H_0 = 2\sqrt{2}, a_0 = 0.6$. It has been shown that the upscale flux divergence is insensitive to many details of the wave train (Biello and Majda 2005). Thus we pick the cosine function for the wavelike structure for the synoptic scale fluctuations. $\lambda = 0.65$ measures the typical length scale of the wave packet and $\phi(T)$is for the time varying phases of the convective supercluster. α is the ratio of stratiform to deep convective heating and $x_0 = 0.5$ is phase difference between the stratiform and deep convective heating.

d. the heating profile in the MJO model at the section 4c

In the MJO model in Eq.12, the envelope function of the heating $F(X - sT)$, the meridional profile $H(y)$ and the relative strength of the second baroclinic mode are chosen as follows,

$$F(X - sT) = A_0 \cos\left[\frac{\pi (X - sT)}{2L_F}\right]^+ ; H(y) = H_0 e^{-(y - y_0)^2} ; \alpha (X - sT) = \frac{3(X - sT)}{2L_F} \qquad \text{(B4)}$$

here $A_0 = 1.08$ is the magnitude of the convective envelope. $L = 1/3$ represents 5000 km half width of the envelope. $s = 0.1$ corresponds to $5ms^{-1}$, $H_0 = 2$. The maximum value for the meridional profile $y_0 = -0.8$ is chosen so that the heating reaches maximum value south of the equator to mimic the boreal winter case. The envelope function is nonzero only in the domain $-L < X - st < L$, thus the relative strength coefficient α varies in the range $[-3/2, 3/2]$.

APPENDIX C

the synoptic-scale equatorial weak temperature gradient (SEWTG) equations

The SEWTG equations was first established based on the systematic derivation of the intraseasonal planetary equatorial synoptic dynamics (IPESD)model from the primitive equations (Majda and Klein 2003).Then they are utilized for wave trains of thermally driven equatorial synoptic-scale circulations in a multi-scale model for the MJO (Majda and Biello 2004; Biello and Majda 2005, 2006). The equations, in dimensionless units, read as follows,

$$-yv' + p'_x = 0 \tag{C1a}$$

$$yu' + p'_y = 0 \tag{C1b}$$

$$w' = S'_\theta \tag{C1c}$$

$$p'_z = \theta' \tag{C1d}$$

$$u'_x + v'_y + w'_z = 0 \tag{C1e}$$

here all physical variables including the synoptic heating has zero mean on the synoptic scales.

References

Benedict, J. J., and D. A. Randall, 2011: Impacts of idealized air-sea coupling on madden-julian oscillation structure in the superparameterized cam. *Journal of the Atmospheric Sciences*, **68 (9)**, 1990–2008.

Biello, J. A., and A. J. Majda, 2005: A new multiscale model for the madden–julian oscillation. *Journal of the atmospheric sciences*, **62 (6)**, 1694–1721.

Biello, J. A., and A. J. Majda, 2006: Modulating synoptic scale convective activity and boundary layer dissipation in the ipesd models of the madden–julian oscillation. *Dynamics of atmospheres and oceans*, **42 (1)**, 152–215.

Chen, S. S., and R. A. Houze, 1997: Diurnal variation and life-cycle of deep convective systems over the tropical pacific warm pool. *Quarterly Journal of the Royal Meteorological Society*, **123 (538)**, 357–388.

Dai, A., and K. E. Trenberth, 2004: The diurnal cycle and its depiction in the community climate system model. *Journal of climate*, **17 (5)**, 930–951.

Frenkel, Y., B. Khouider, and A. J. Majda, 2011a: Simple multicloud models for the diurnal cycle of tropical precipitation. part i: Formulation and the case of the tropical oceans. *Journal of the Atmospheric Sciences*, **68 (10)**, 2169–2190.

Frenkel, Y., B. Khouider, and A. J. Majda, 2011b: Simple multicloud models for the diurnal cycle of tropical precipitation. part i: Formulation and the case of the tropical oceans. *Journal of the Atmospheric Sciences*, **68 (10)**, 2169–2190.

Frenkel, Y., B. Khouider, and A. J. Majda, 2011c: Simple multicloud models for the diurnal cycle of tropical precipitation. part ii: the continental regime. *Journal of the Atmospheric Sciences*, **68 (10)**, 2192–2207.

Frenkel, Y., B. Khouider, and A. J. Majda, 2011d: Simple multicloud models for the diurnal cycle of tropical precipitation. part ii: The continental regime. *Journal of the Atmospheric Sciences*, **68 (10)**, 2192–2207.

Frenkel, Y., A. J. Majda, and B. Khouider, 2013: Simple models for the diurnal cycle and convectively coupled waves. *Theoretical and Computational Fluid Dynamics*, **27 (3-4)**, 533–559.

Gill, A., 1980: Some simple solutions for heat-induced tropical circulation. *Quarterly Journal of the Royal Meteorological Society*, **106 (449)**, 447–462.

Hendon, H. H., and M. L. Salby, 1994: The life cycle of the madden-julian oscillation. *Journal of the Atmospheric Sciences*, **51 (15)**, 2225–2237.

Hendon, H. H., and K. Woodberry, 1993: The diurnal cycle of tropical convection. *Journal of Geophysical Research: Atmospheres (1984–2012)*, **98 (D9)**, 16 623–16 637.

Inness, P. M., and J. M. Slingo, 2003: Simulation of the madden-julian oscillation in a coupled general circulation model. part i: Comparison with observations and an atmosphere-only gcm. *Journal of Climate*, **16 (3)**, 345–364.

Khairoutdinov, M., D. Randall, and C. DeMott, 2005: Simulations of the atmospheric general circulation using a cloud-resolving model as a superparameterization of physical processes. *Journal of the Atmospheric Sciences*, **62 (7)**, 2136–2154.

Khouider, B., and A. J. Majda, 2006a: Model multi-cloud parameterizations for convectively coupled waves: Detailed nonlinear wave evolution. *Dynamics of atmospheres and oceans*, **42 (1)**, 59–80.

Khouider, B., and A. J. Majda, 2006b: Multicloud convective parametrizations with crude vertical structure. *Theoretical and Computational Fluid Dynamics*, **20 (5-6)**, 351–375.

Khouider, B., and A. J. Majda, 2006c: A simple multicloud parameterization for convectively coupled tropical waves. part i: Linear analysis. *Journal of the atmospheric sciences*, **63 (4)**, 1308–1323.

Khouider, B., and A. J. Majda, 2007: A simple multicloud parameterization for convectively coupled tropical waves. part ii: Nonlinear simulations. *Journal of the atmospheric sciences*, **64 (2)**, 381–400.

Khouider, B., and A. J. Majda, 2008a: Equatorial convectively coupled waves in a simple multicloud model. *Journal of the Atmospheric Sciences*, **65 (11)**, 3376–3397.

Khouider, B., and A. J. Majda, 2008b: Multicloud models for organized tropical convection: Enhanced congestus heating. *Journal of the Atmospheric Sciences*, **65 (3)**, 895–914.

Kikuchi, K., and B. Wang, 2008: Diurnal precipitation regimes in the global tropics*. *Journal of Climate*, **21 (11)**, 2680–2696.

Kiladis, G. N., K. H. Straub, and P. T. Haertel, 2005: Zonal and vertical structure of the madden-julian oscillation. *Journal of the Atmospheric Sciences*, **62 (8)**, 2790–2809.

Lin, J.-L., M. Zhang, and B. Mapes, 2005: Zonal momentum budget of the madden-julian oscillation: The source and strength of equivalent linear damping. *Journal of the atmospheric sciences*, **62 (7)**, 2172–2188.

Lin, X., and R. H. Johnson, 1996: Kinematic and thermodynamic characteristics of the flow over the western pacific warm pool during toga coare. *Journal of the atmospheric sciences*, **53 (5)**, 695–715.

Majda, A. J., 2007: New multiscale models and self-similarity in tropical convection. *Journal of the atmospheric sciences*, **64 (4)**, 1393–1404.

Majda, A. J., and J. A. Biello, 2004: A multiscale model for tropical intraseasonal oscillations. *Proceedings of the National Academy of Sciences of the United States of America*, **101 (14)**, 4736–4741.

Majda, A. J., and R. Klein, 2003: Systematic multiscale models for the tropics. *Journal of the Atmospheric Sciences*, **60 (2)**, 393–408.

Mapes, B. E., and R. A. Houze Jr, 1995: Diabatic divergence profiles in western pacific mesoscale convective systems. *Journal of the atmospheric sciences*, **52 (10)**, 1807–1828.

Matsuno, T., 1966: Quasi-geostrophic motions in the equatorial area. *J. Meteor. Soc. Japan*, **44 (1)**, 25–43.

Neale, R., and J. Slingo, 2003: The maritime continent and its role in the global climate: A gcm study. *Journal of Climate*, **16 (5)**, 834–848.

Peatman, S. C., A. J. Matthews, and D. P. Stevens, 2014: Propagation of the madden–julian oscillation through the maritime continent and scale interaction with the diurnal cycle of precipitation. *Quarterly Journal of the Royal Meteorological Society*, **140 (680)**, 814–825.

Ramage, C. S., 1968: Role of a tropical maritime continent in the atmospheric circulation 1. *Monthly Weather Review*, **96 (6)**, 365–370.

Randall, D. A., and D. A. Dazlich, 1991: Diurnal variability of the hydrologic cycle in a general circulation model. *Journal of the Atmospheric Sciences*, **48 (1)**, 40–62.

Rauniyar, S. P., and K. J. Walsh, 2011: Scale interaction of the diurnal cycle of rainfall over the maritime continent and australia: Influence of the mjo. *Journal of Climate*, **24 (2)**, 325–348.

Raupp, C. F., and P. L. Silva Dias, 2009: Resonant wave interactions in the presence of a diurnally varying heat source. *Journal of the Atmospheric Sciences*, **66 (10)**, 3165–3183.

Raupp, C. F., and P. L. Silva Dias, 2010: Interaction of equatorial waves through resonance with the diurnal cycle of tropical heating. *Tellus A*, **62 (5)**, 706–718.

Ray, C., 1928: Diurnal variation of rainfall at san juan, pr 1. *Monthly Weather Review*, **56 (4)**, 140–141.

Romps, D. M., 2014: Rayleigh damping in the free troposphere. *Journal of the Atmospheric Sciences*, **71 (2)**, 553–565.

Rui, H., and B. Wang, 1990: Development characteristics and dynamic structure of tropical intraseasonal convection anomalies. *Journal of the Atmospheric Sciences*, **47 (3)**, 357–379.

Slingo, J., P. Inness, R. Neale, S. Woolnough, and G. Yang, 2003: Scale interactions on diurnal toseasonal timescales and their relevanceto model systematic errors. *Annals of Geophysics*.

Sobel, A. H., J. Nilsson, and L. M. Polvani, 2001: The weak temperature gradient approximation and balanced tropical moisture waves. *Journal of the atmospheric sciences*, **58 (23)**, 3650–3665.

Sperber, K. R., J. Slingo, P. Inness, and W.-M. Lau, 1997: On the maintenance and initiation of the intraseasonal oscillation in the ncep/ncar reanalysis and in the gla and ukmo amip simulations. *Climate Dynamics*, **13 (11)**, 769–795.

Sui, C., and K. Lau, 1992: Multiscale phenomena in the tropical atmosphere over the western pacific. *Monthly weather review*, **120 (3)**, 407–430.

Sui, C., X. Li, K. Lau, and D. Adamec, 1997: Multiscale air-sea interactions during toga coare. *Monthly weather review*, **125 (4)**, 448–462.

Tian, B., B. J. Soden, and X. Wu, 2004: Diurnal cycle of convection, clouds, and water vapor in the tropical upper troposphere: Satellites versus a general circulation model. *Journal of Geophysical Research: Atmospheres (1984–2012)*, **109 (D10)**.

Tian, B., D. E. Waliser, and E. J. Fetzer, 2006: Modulation of the diurnal cycle of tropical deep convective clouds by the mjo. *Geophysical research letters*, **33 (20)**.

Tung, W.-w., D. Giannakis, and A. J. Majda, 2014: Symmetric and antisymmetric convection signals in the madden–julian oscillation. part i: basic modes in infrared brightness temperature. *Journal of the Atmospheric Sciences*, **71 (9)**, 3302–3326.

Waliser, D., and W. K.-M. Lau, 2005: Intraseasonal variability in the atmosphere-ocean climate system. *Intraseasonal Variability in the Atmosphere-Ocean Climate System, by D. Waliser and WK-M. Lau. 2005 XVIII, 474 p. 80 illus. 3-540-22276-6. Berlin: Springer, 2005.*, **1**.

Wu, C.-H., and H.-H. Hsu, 2009: Topographic influence on the mjo in the maritime continent. *Journal of Climate*, **22 (20)**, 5433–5448.

Yanai, M., B. Chen, and W.-w. Tung, 2000: The madden-julian oscillation observed during the toga coare iop: Global view. *Journal of the atmospheric sciences*, **57 (15)**, 2374–2396.

Yang, G.-Y., and J. Slingo, 2001: The diurnal cycle in the tropics. *Monthly Weather Review*, **129 (4)**, 784–801.

Yang, Q., and A. J. Majda, 2014: A multi-scale model for the intraseasonal impact of the diurnal cycle of tropical convection. *Theoretical and Computational Fluid Dynamics*, **28 (6)**, 605–633.

Zhang, C., 2005: Madden-julian oscillation. *Reviews of Geophysics*, **43 (2)**.

LIST OF TABLES

TABLE 1. The dimensional units for all physical variables and some constant parameters. Here square brackets mean the value of one unit of the dimensionless variables corresponding to the given scale.

Physical quantity	Mathematical symbol	Value
Froude number	ε	0.1
Gravity wave speed	c	$50m/s$
Brunt-vaisala frequency	N	$0.01s^{-1}$
Troposphere height	H_T	$16km$
Equatorial time scale	T_E	$(c\beta)^{-1/2} = 8.3h$
Equatorial deformation radius	L_E	$(c/\beta)^{1/2} = 1500km$
Synoptic scale	$[x, y]$	$L_E = 1500km$
vertical scale	$[z]$	$H_T/\pi = 5km$
Daily scale	$[t]$	$T_E = 8.3h$
Zonal planetary scale	$[X]$	$L_P = L_E/\varepsilon = 15000km$
Intraseasonal scale	$[T]$	$T_I = T_E/\varepsilon = 3.5day$
Horizontal velocity	$\tilde{u}, \tilde{v}$	$5ms^{-1}$
Vertical velocity	$\tilde{w}$	$1.6cms^{-1}$
Potential temperature anomaly	$\tilde{\theta}$	$1.53K$
Zonal velocity on the intraseasonal time scale	U	$5ms^{-1}$
Meridional velocity on the intraseasonal time scale	V	$0.5ms^{-1}$
Vertical velocity on the intraseasonal time scale	W	$0.16cms^{-1}$
Potential temperature anomaly on the intraseasonal time scale	Θ	$1.53K$
Momentum dissipation coefficient	d	$1/7$days
Radiative cooling coefficient	d_θ	$1/7$ days

LIST OF FIGURES

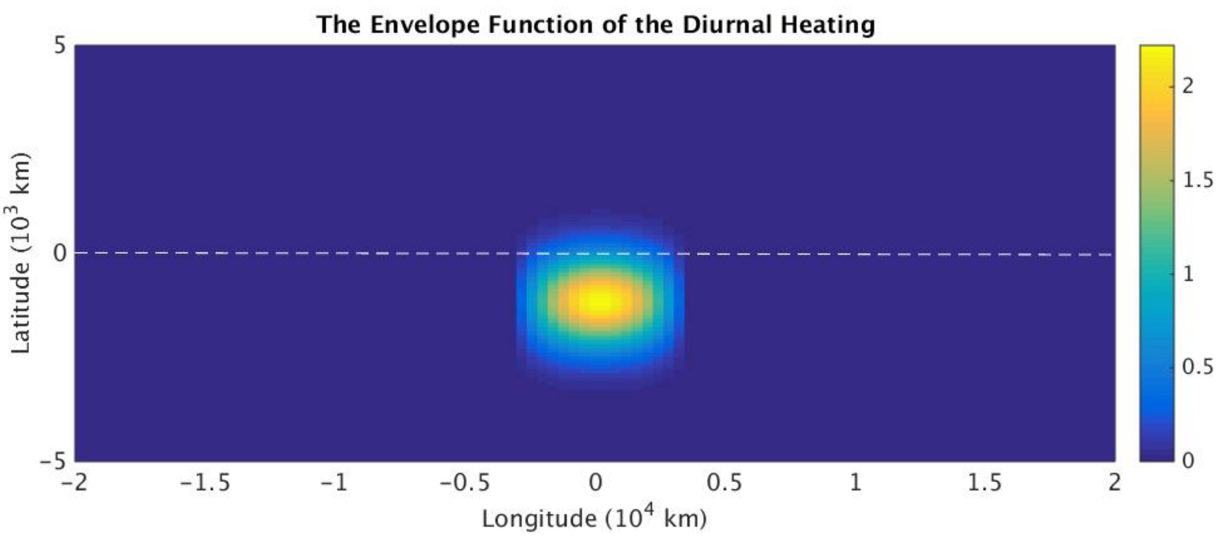

970 FIG. 1. The envelope function of the diurnal heating in longitude-latitude diagram during boreal winter. The
971 value here is dimensionless. This mimics the localized effect of the Martime Continent in the model.

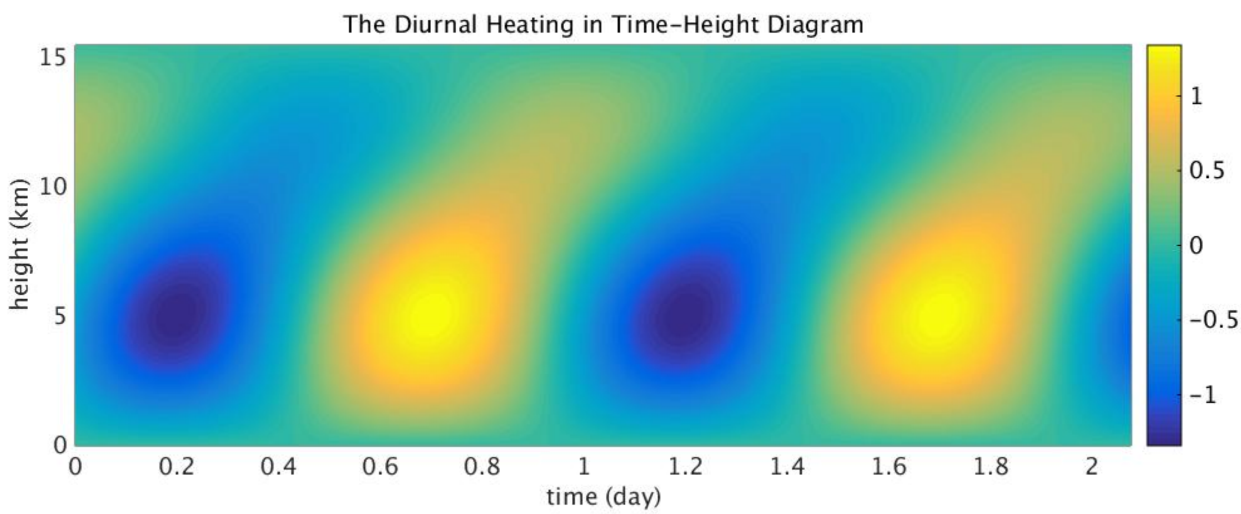

FIG. 2. The diurnal heating in time-height diagram during boreal winter. The value is dimentionless.

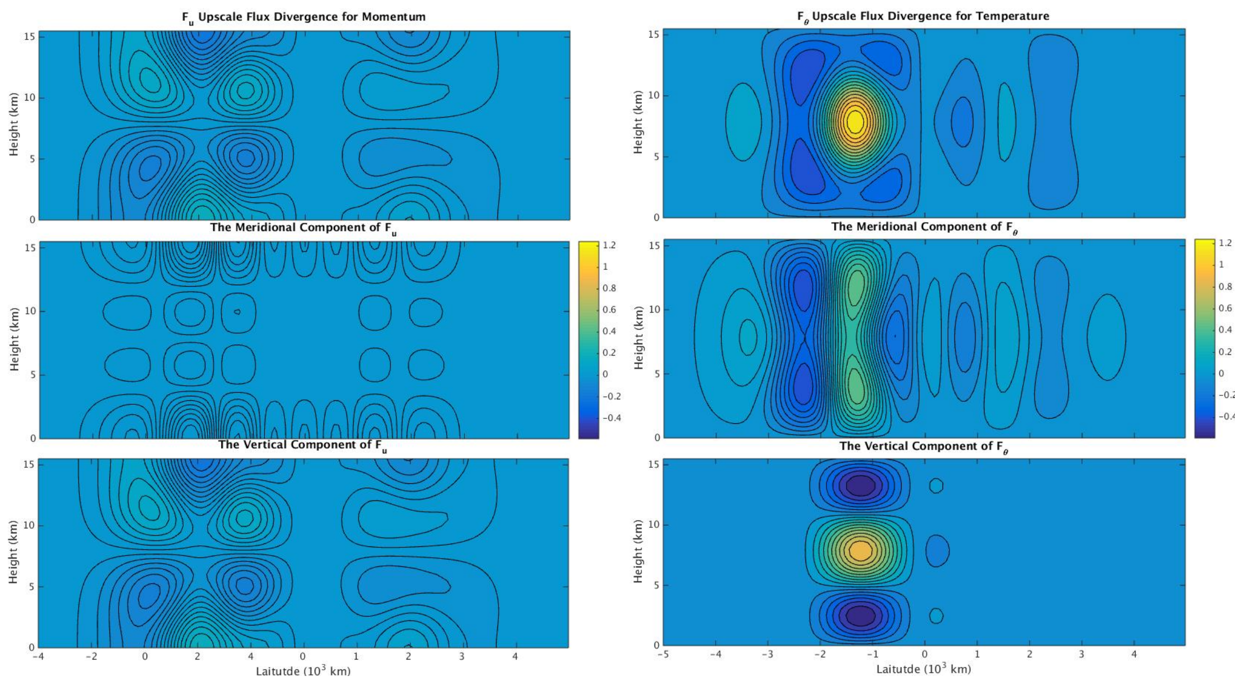

FIG. 3. The eddy flux divergences of momentum and temperature F^u, F^θ in the latitude-height diagram during boreal winter. The left panels from top to bottom show eddy flux divergence of momentum F^u, its meridional component $-\frac{\partial}{\partial y}\langle\tilde{v}\tilde{u}\rangle$ and its vertical component $-\frac{\partial}{\partial z}\langle\tilde{w}\tilde{u}\rangle$. The right panels from top to bottom show eddy flux divergence of temperature F^θ, its meridional component $-\frac{\partial}{\partial y}\langle\tilde{v}\tilde{\theta}\rangle$ and its vertical component $-\frac{\partial}{\partial z}\langle\tilde{w}\tilde{\theta}\rangle$. One dimensionless unit of F^u is $1m/s/day$ and that of $F^\theta$is $0.45K/day$.

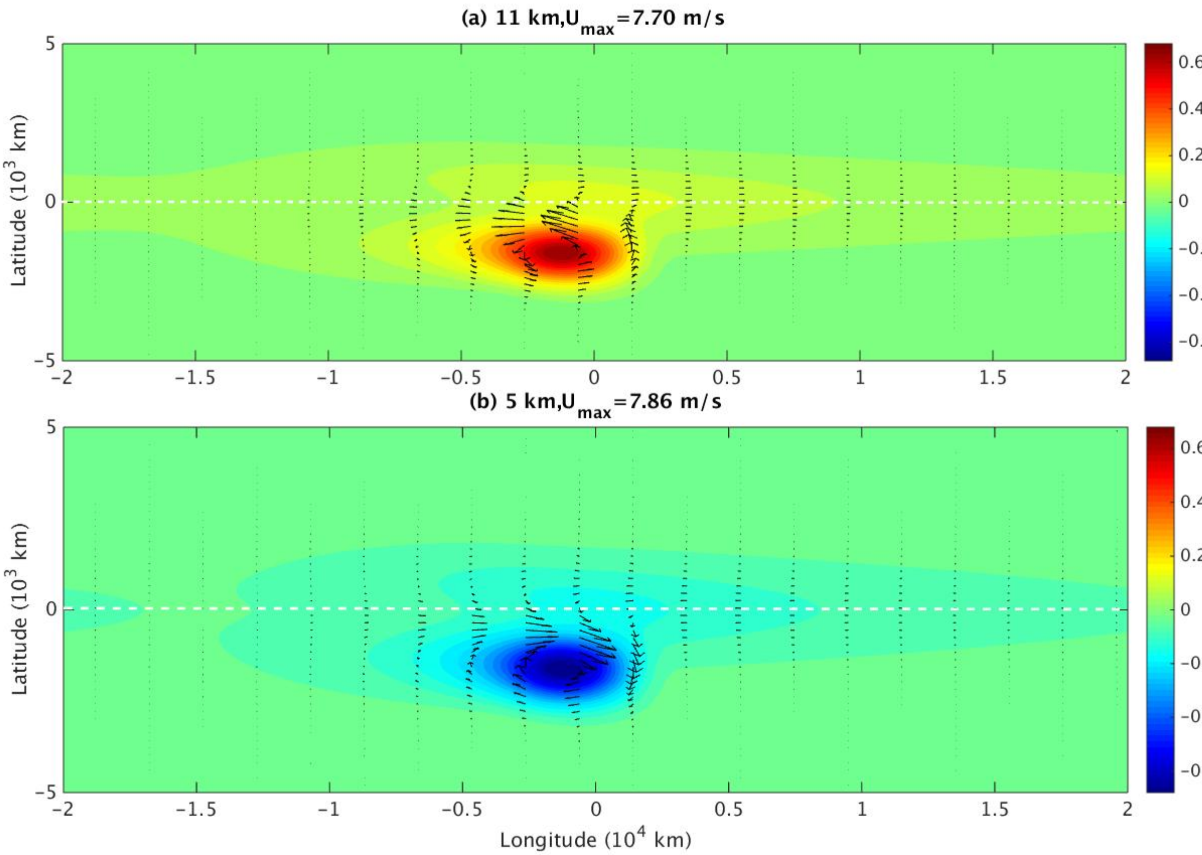

977 FIG. 4. The horizontal flow field (shown by vectors) and pressure anomaly (shown by color) due to the
978 intraseasonal impact of the diurnal cycle. The height in the top panel and bottom panels are 11 km and 5 km,
979 respectively. The unit of pressure anomaly is $250m^2s^{-2}$.

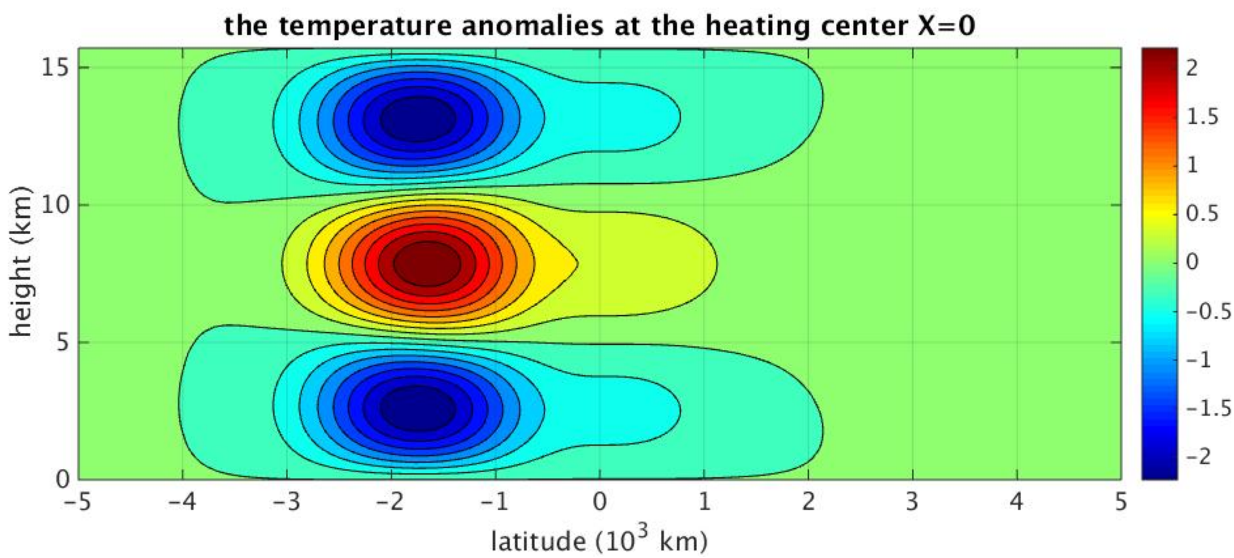

FIG. 5. The temperature anomaly at the latitude-height diagram due to the intraseasonal impact of the diurnal cycle. The red color means warm and blue color means cold. The unit of temperature anomaly is K.

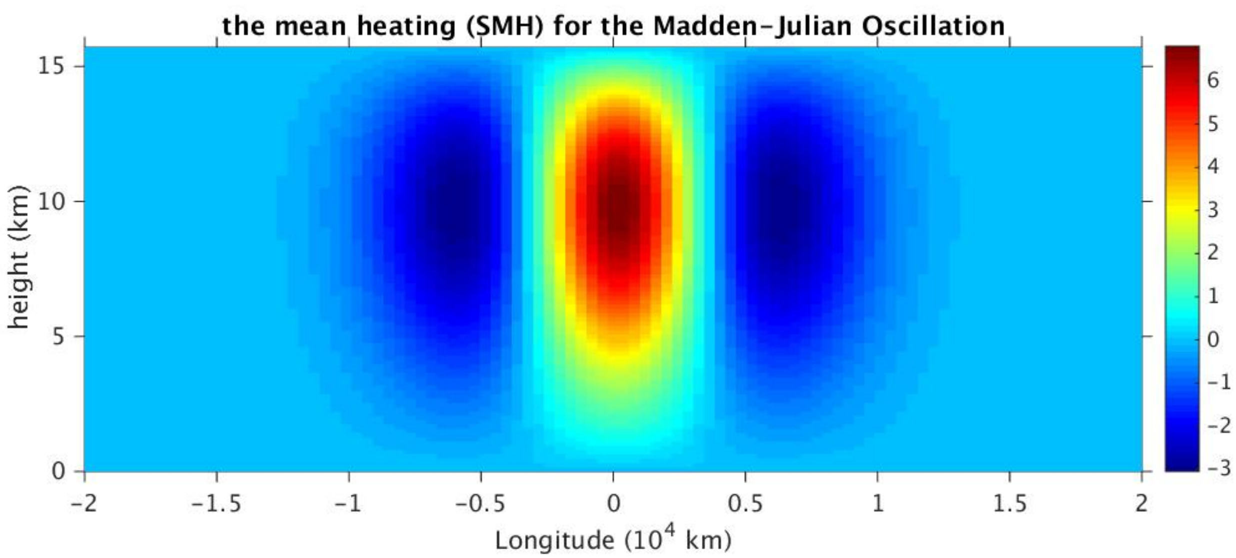

982 FIG. 6. The mean heating (SMH) for the Madden-Julian Oscillation. The red color means heating and blue
983 color means cooling. The unit of the heating is $4.5K/day$

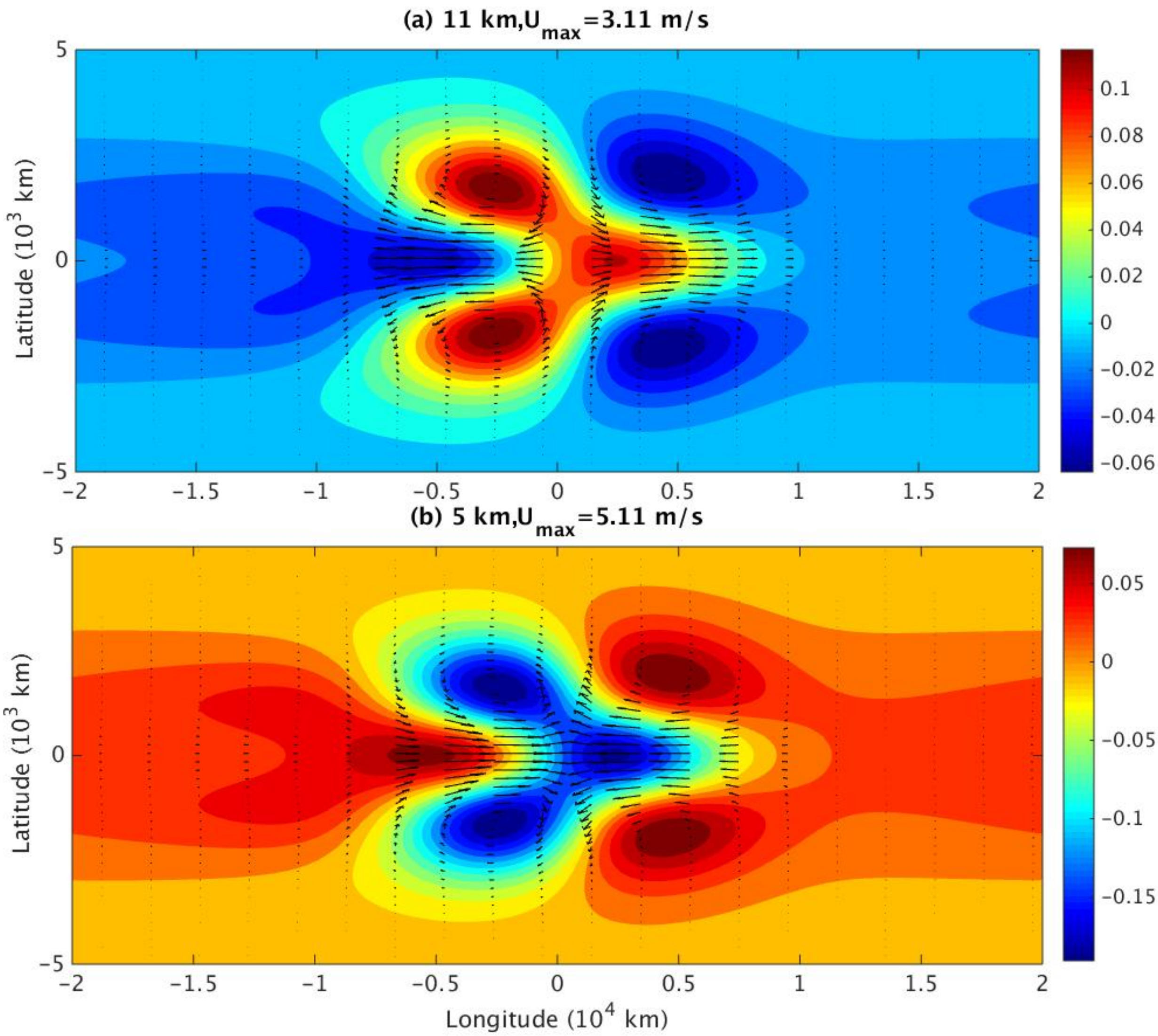

984 FIG. 7. The horizontal flow field (shown by vectors) and pressure anomaly (shown by color) forced by the
985 standard mean heating(SMH). The top panel shows the flow field at height z=11 km. The bottom panel is for
986 height z=5km. The unit of pressure anomaly is $250 m^2 s^{-2}$.

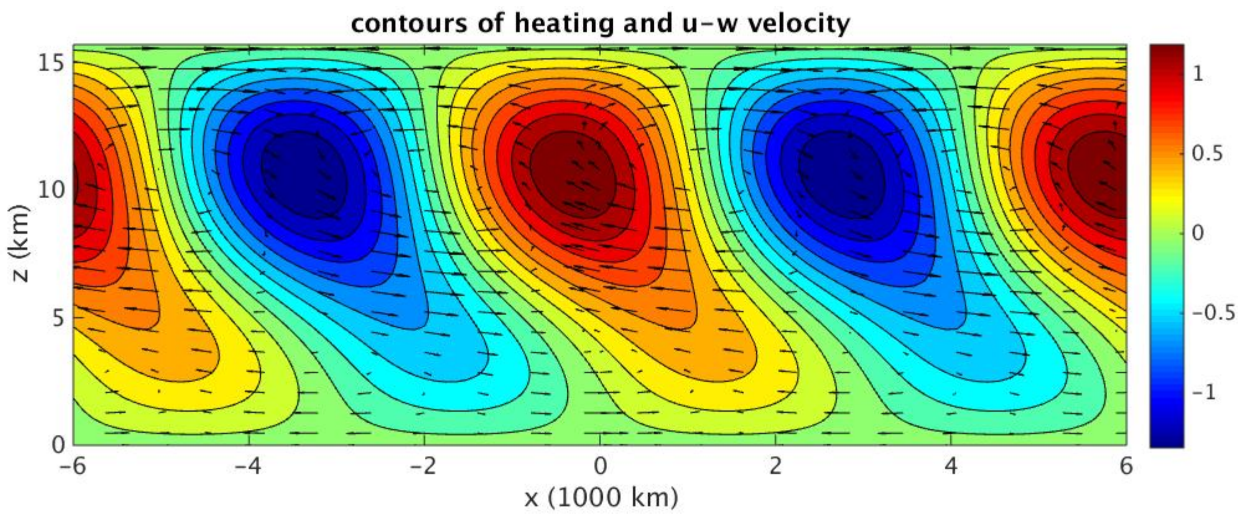

FIG. 8. Contours of synoptic scale heating and vectors of zonal/vertical velocity.

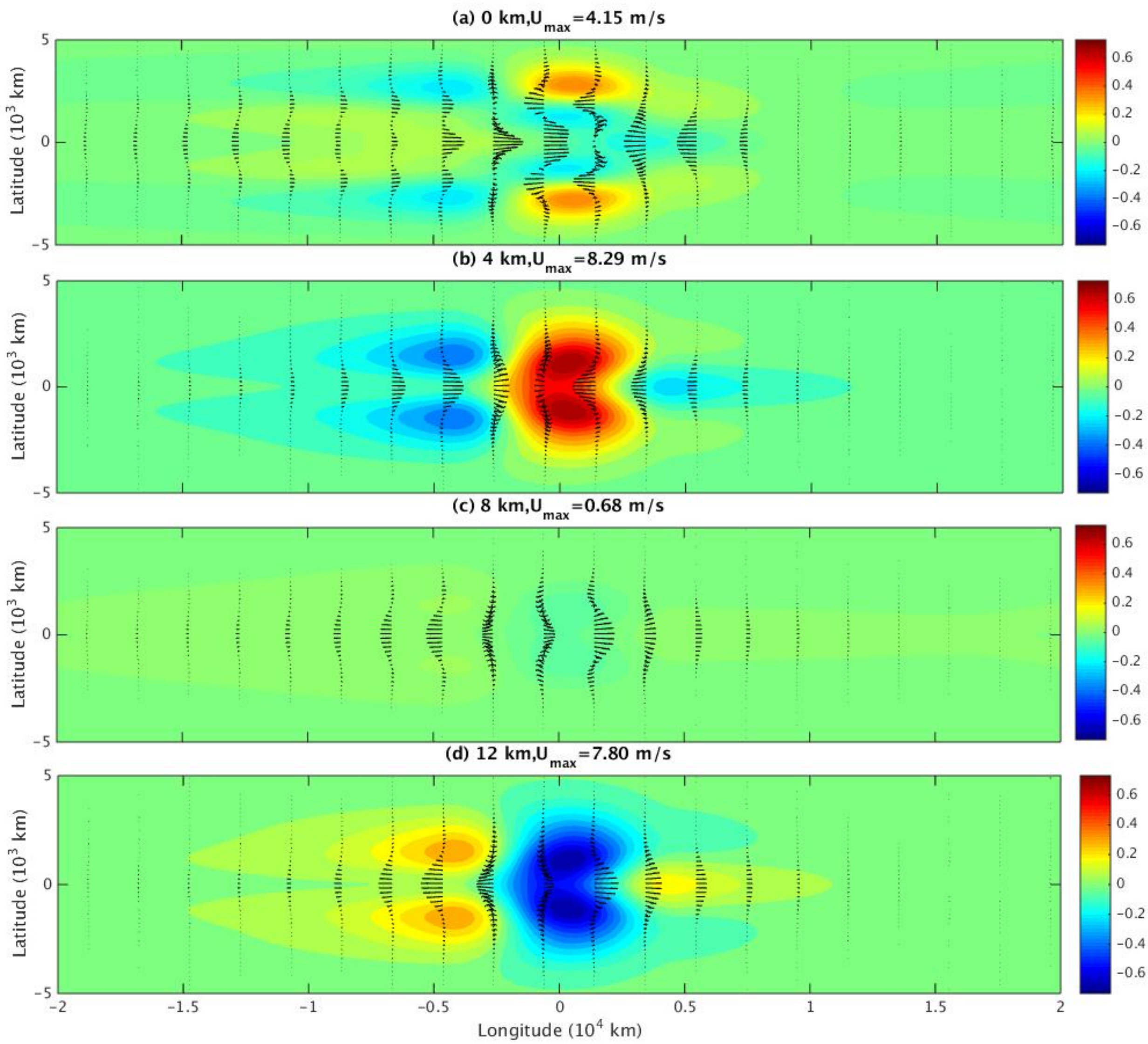

987 FIG. 9. The planetary-scale response to the equatorially symmetric MJO forced by both synoptic-scale heating
988 and mean heating. The color shows pressure perturbation, the flow field is shown by vectors. From top to bottom,
989 these 4 panels show the heights at z=0 km, z=4 km, z=8 km, z=12 km. The pressure anomalies is dimensionless
990 in unit of $250m^2s^{-2}$

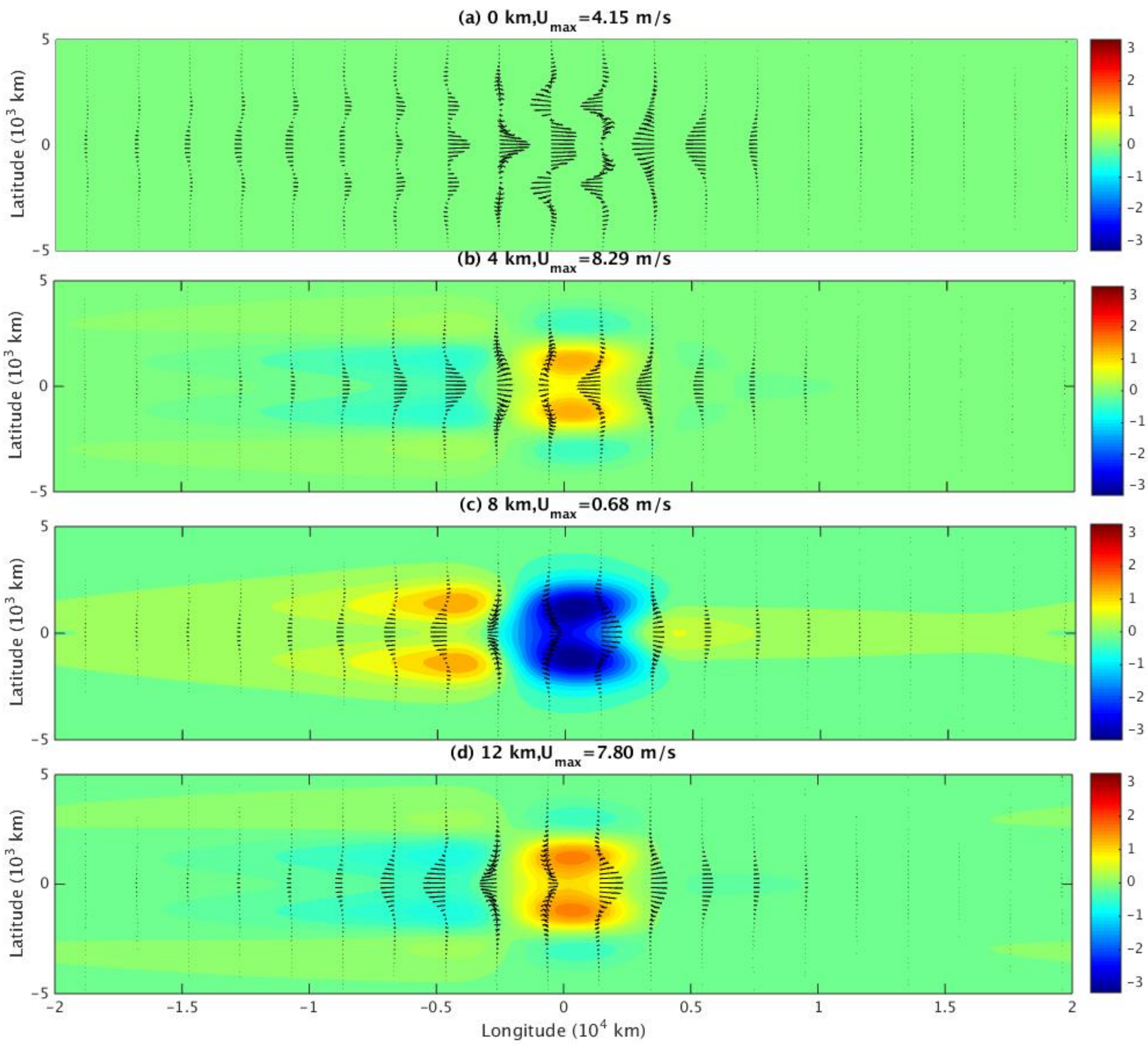

FIG. 10. The planetary-scale response to the equatorially symmetric MJO forced by both synoptic-scale heating and mean heating. The color shows temperature anomaly, the flow field is shown by vectors. From top to bottom, these 4 panels show the heights at z=0 km, z=4 km, z=8 km, z=12 km. The unit of temperature anomaly is K.

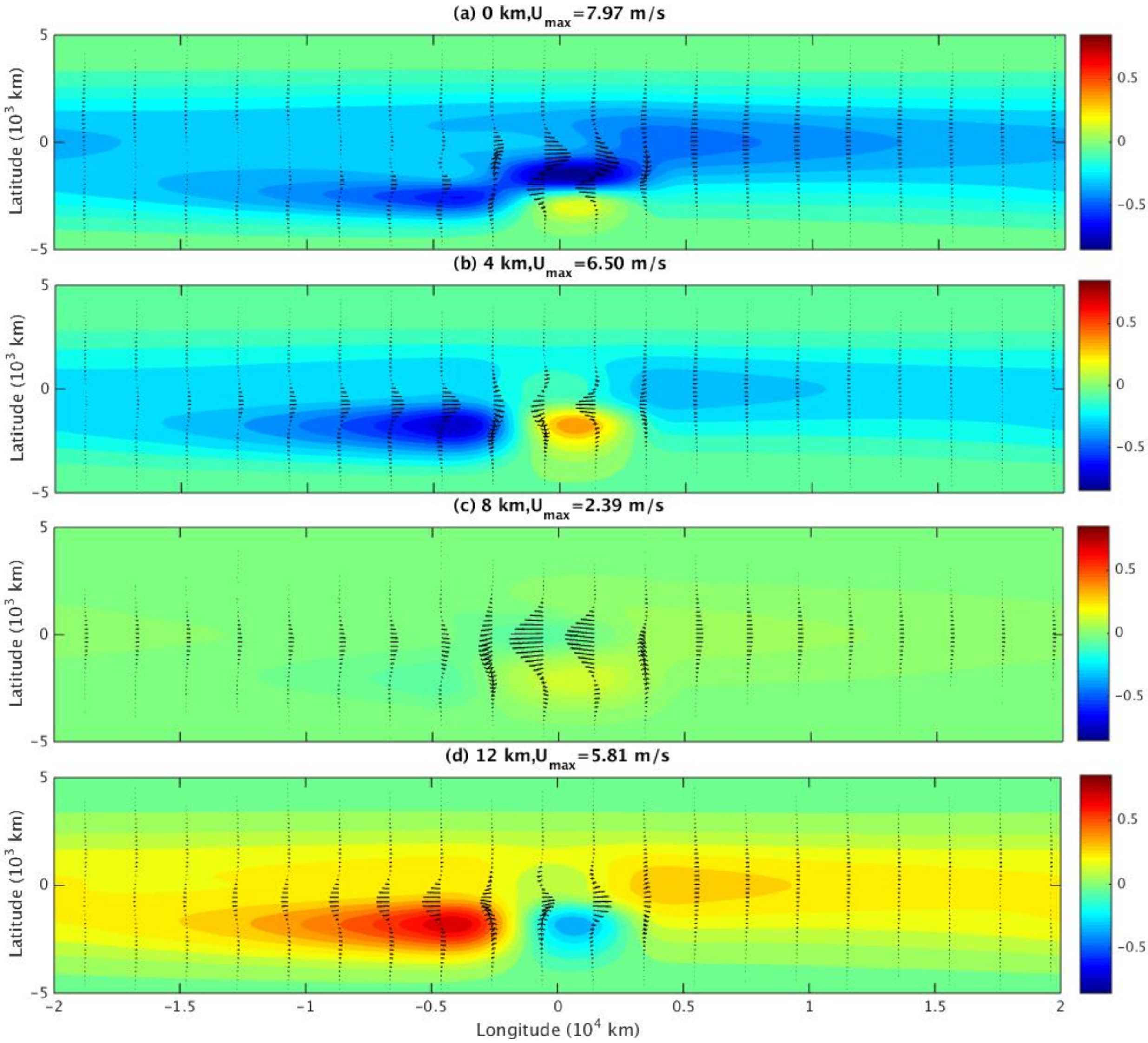

FIG. 11. Planetary-scale response to equatorially asymmetric synoptic-scale and mean heating centered at 900 km south. The panels shows flow vectors, red means positive pressure perturbation, and blue means negative pressure perturbation at heights (a) 0, (b) 4, (c) 8, (d) 12 km. The pressure anomaly is dimensionless.

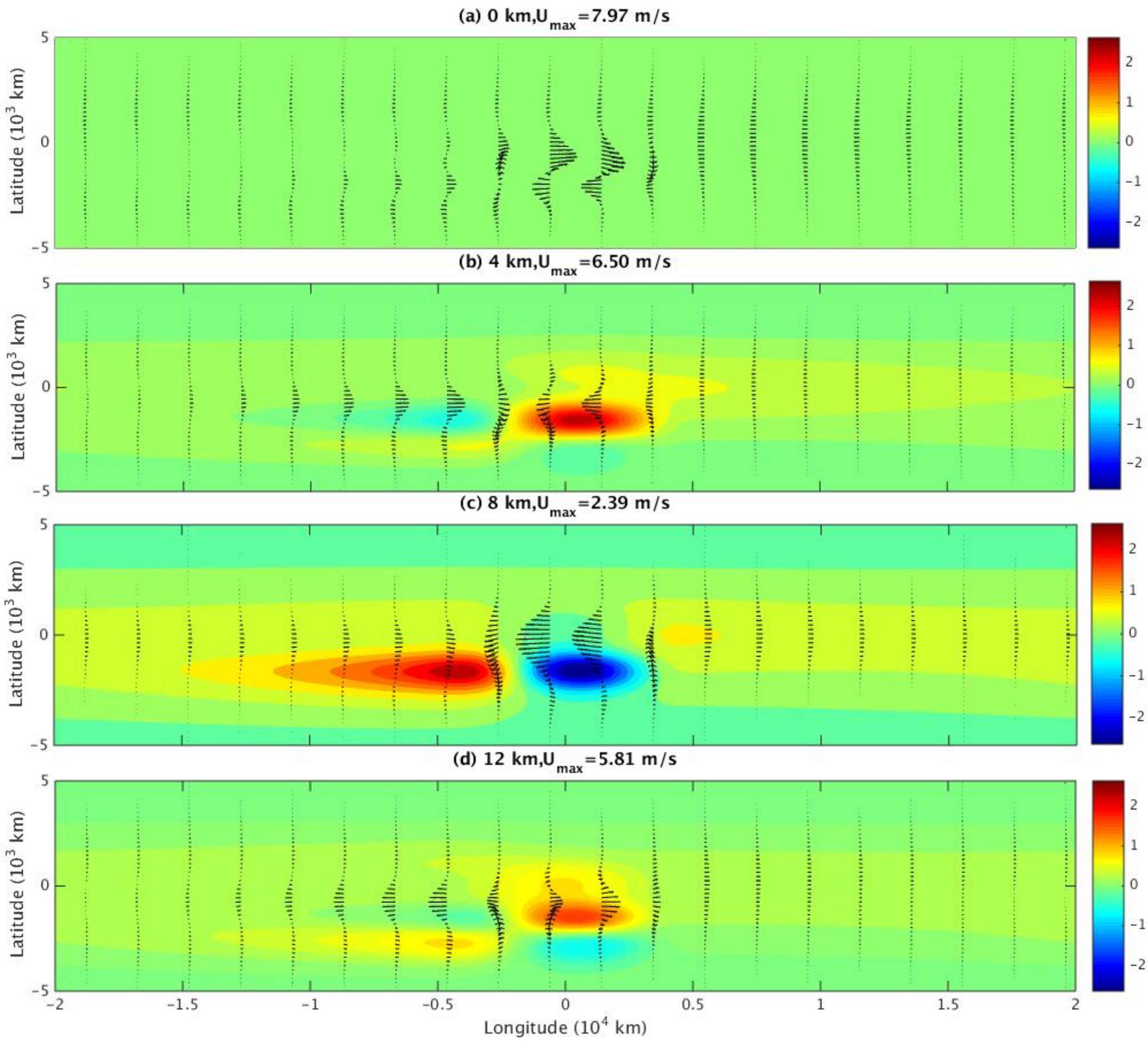

FIG. 12. Planetary-scale response to equatorially asymmetric synoptic-scale and mean heating centered at 900km south. The panels shows flow vectors, red means positive temperature anomaly, and blue means negative temperature anomaly at heights (a) 0, (b) 4, (c) 8, (d) 12 km. The temperature anomaly is in units of K.

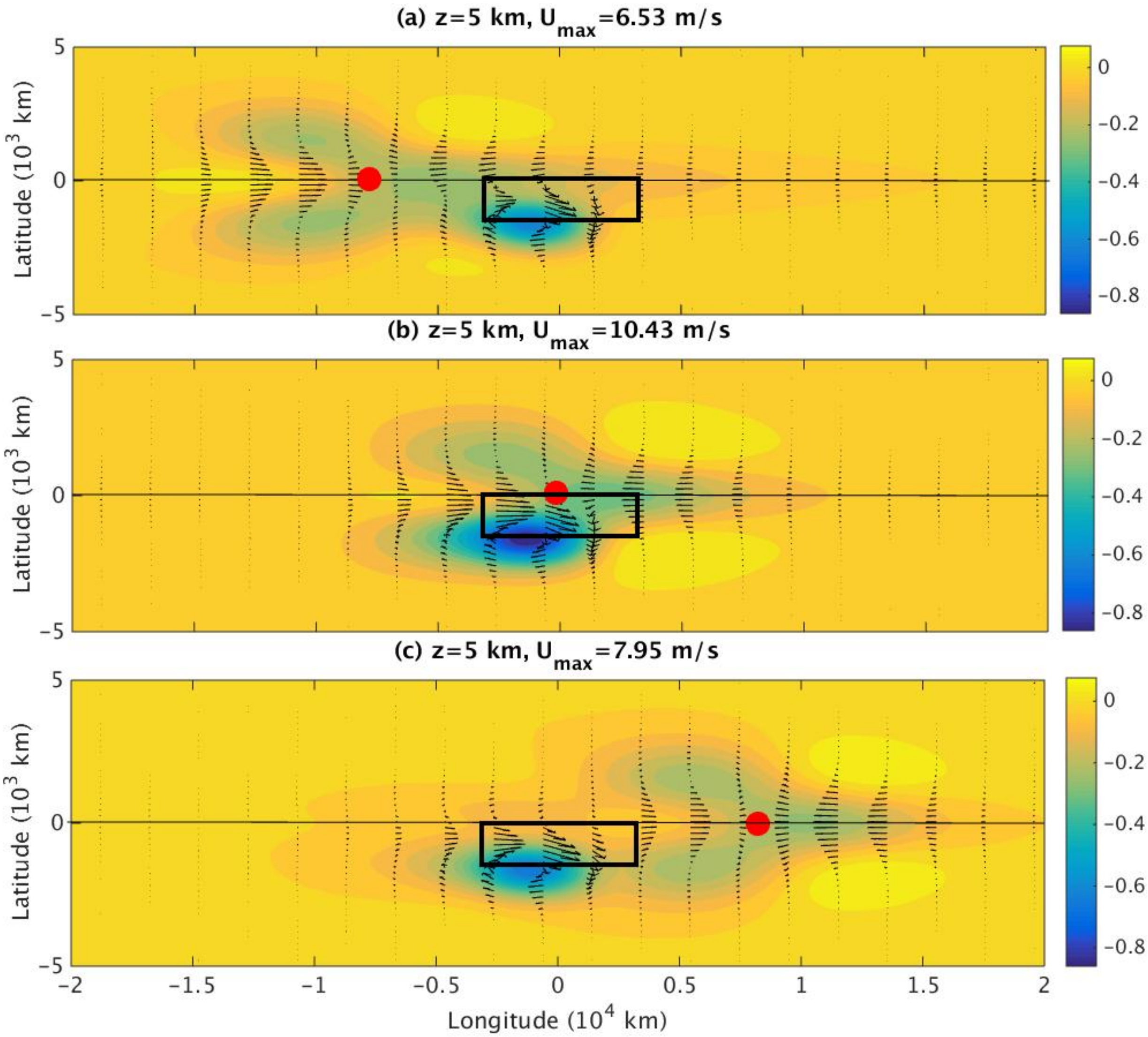

FIG. 13. The horizontal flow field and pressure anomalies at $z = 5\,km$ due to the intraseasonal impact of the diurnal cycle and the MJO. The panels from top to bottom show different phases of MJO. The red circles shows the center of mean heating for MJO. The black box shows the regime where diurnal cycle is significant during boreal winter. The winds direction is shown by vectors and their magnitude is shown by the length of vectors. The pressure anomalies are shown in color.

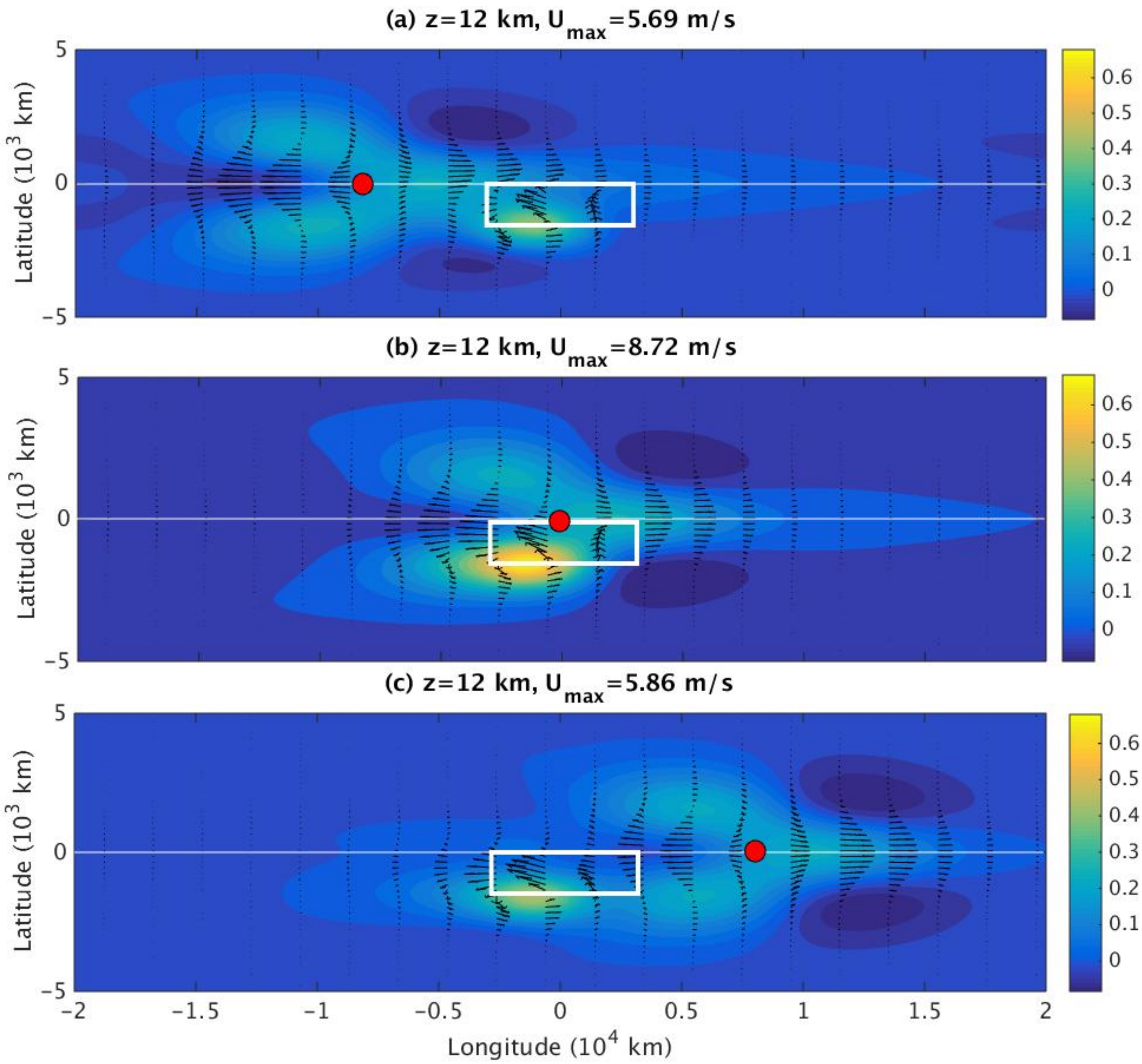

FIG. 14. The horizontal flow field and pressure anomalies at $z = 12\,km$ due to the intraseasonal impact of the diurnal cycle and the MJO. The panels from top to bottom show different phases of MJO. The red circles shows the center of mean heating for MJO. The white box shows the regime where diurnal cycle is significant during boreal winter. The winds direction is shown by vectors and their magnitude is shown by the length of vectors. The pressure anomalies are shown in color.

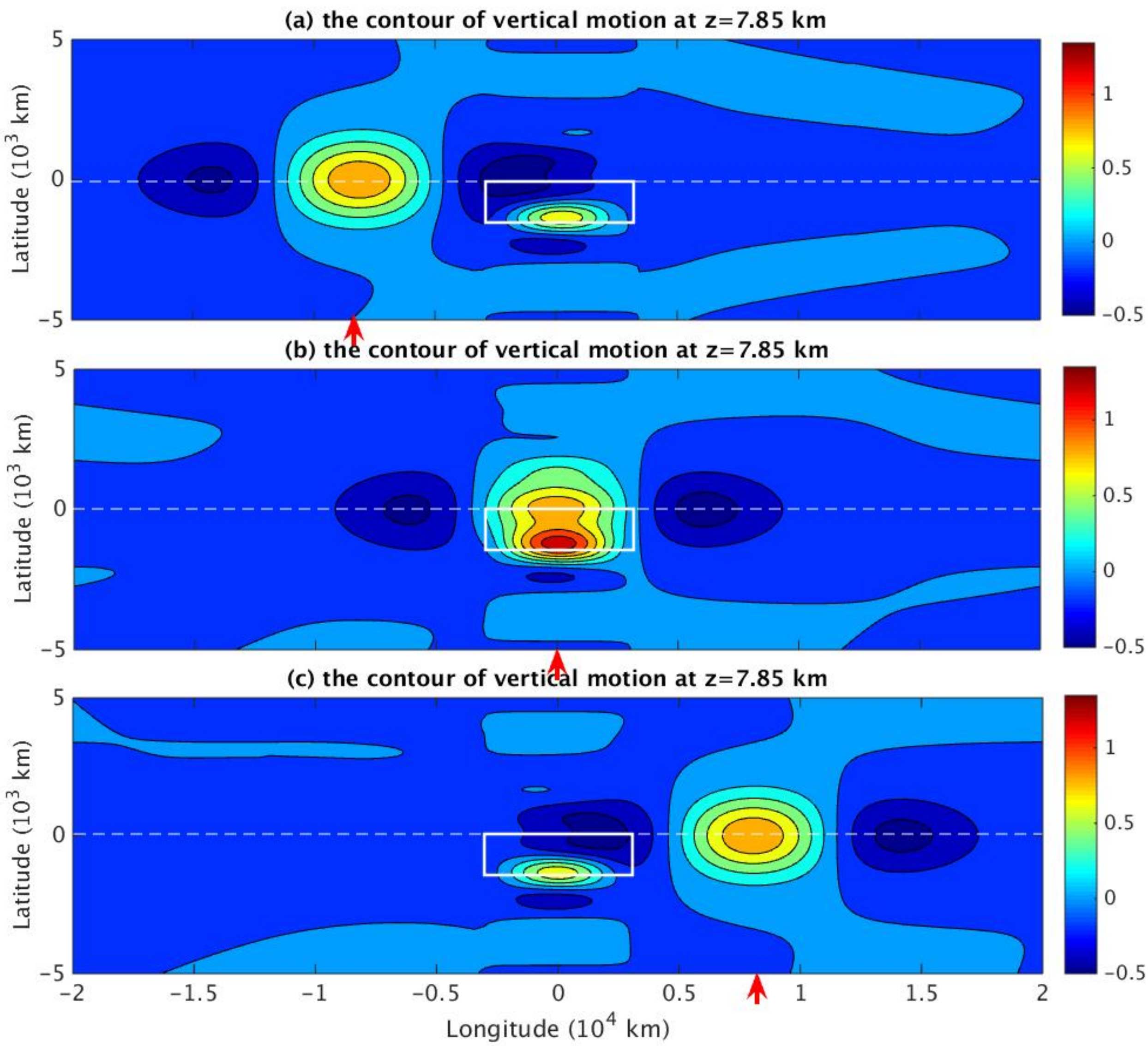

FIG. 15. Contour of vertical motion at the middle troposphere due to the MJO and intraseasonal impact of diurnal cycle. The panels from top to bottom show different phases of MJO. The positive value means rising motion and negative value means sinking motion. The white box shows the location where the diurnal cycle is significant. The red arrow shows the longitude at which the center of MJO convection sits. The unit of vertical velocity is $0.16 cm/s$

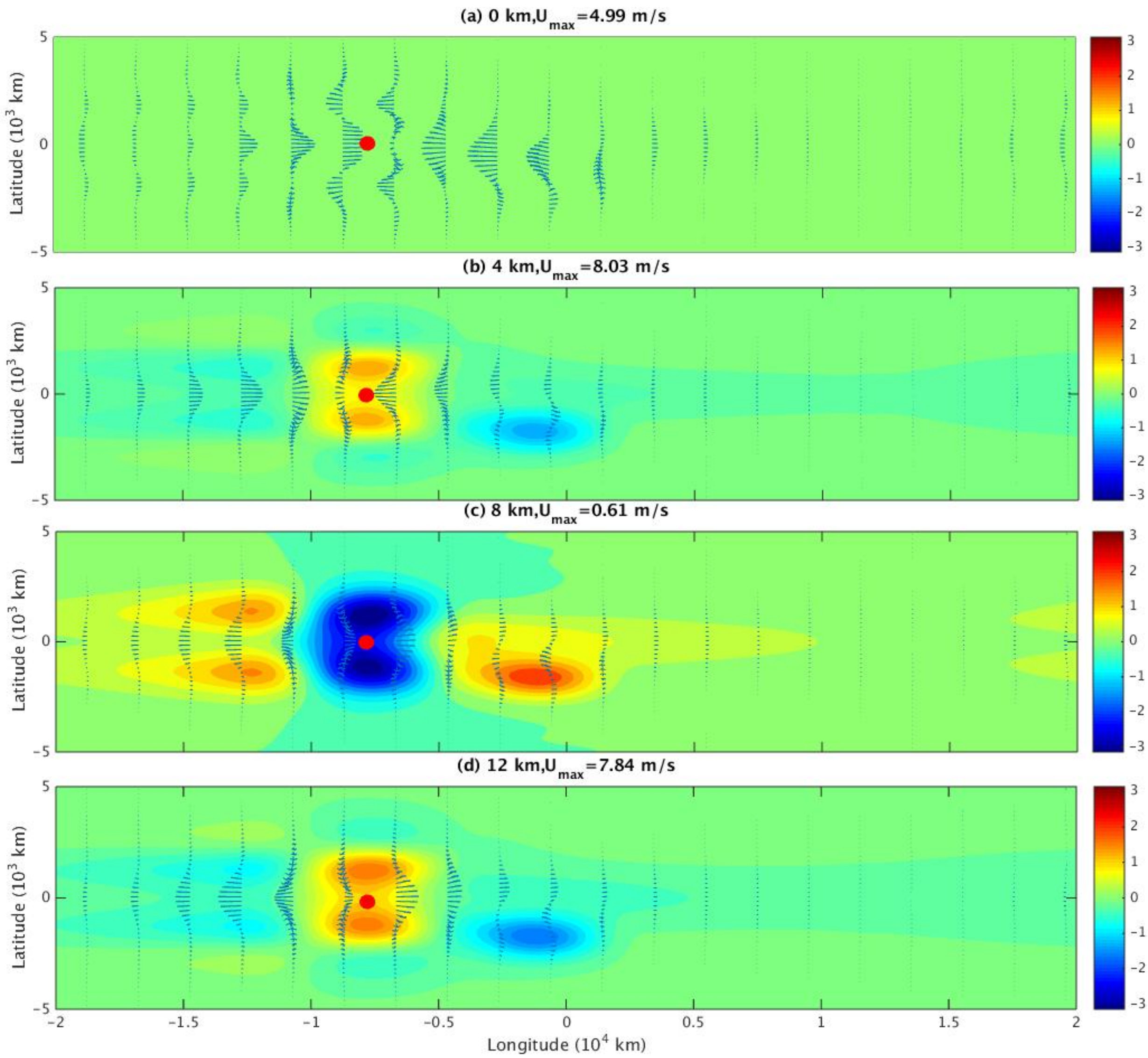

1016 FIG. 16. The temperature anomalies associated with the equatorially symmetric MJO and the intraseasonal
1017 impact of the diurnal cycle at phase I. The color shows temperature anomalies, the flow field is shown by
1018 vectors. From top to bottom, these 4 panels show the heights at z=0 km, z=4 km, z=8 km, z=12 km. The unit of
1019 temperature anomaly is K. The red dot shows the center of the MJO convective activities.

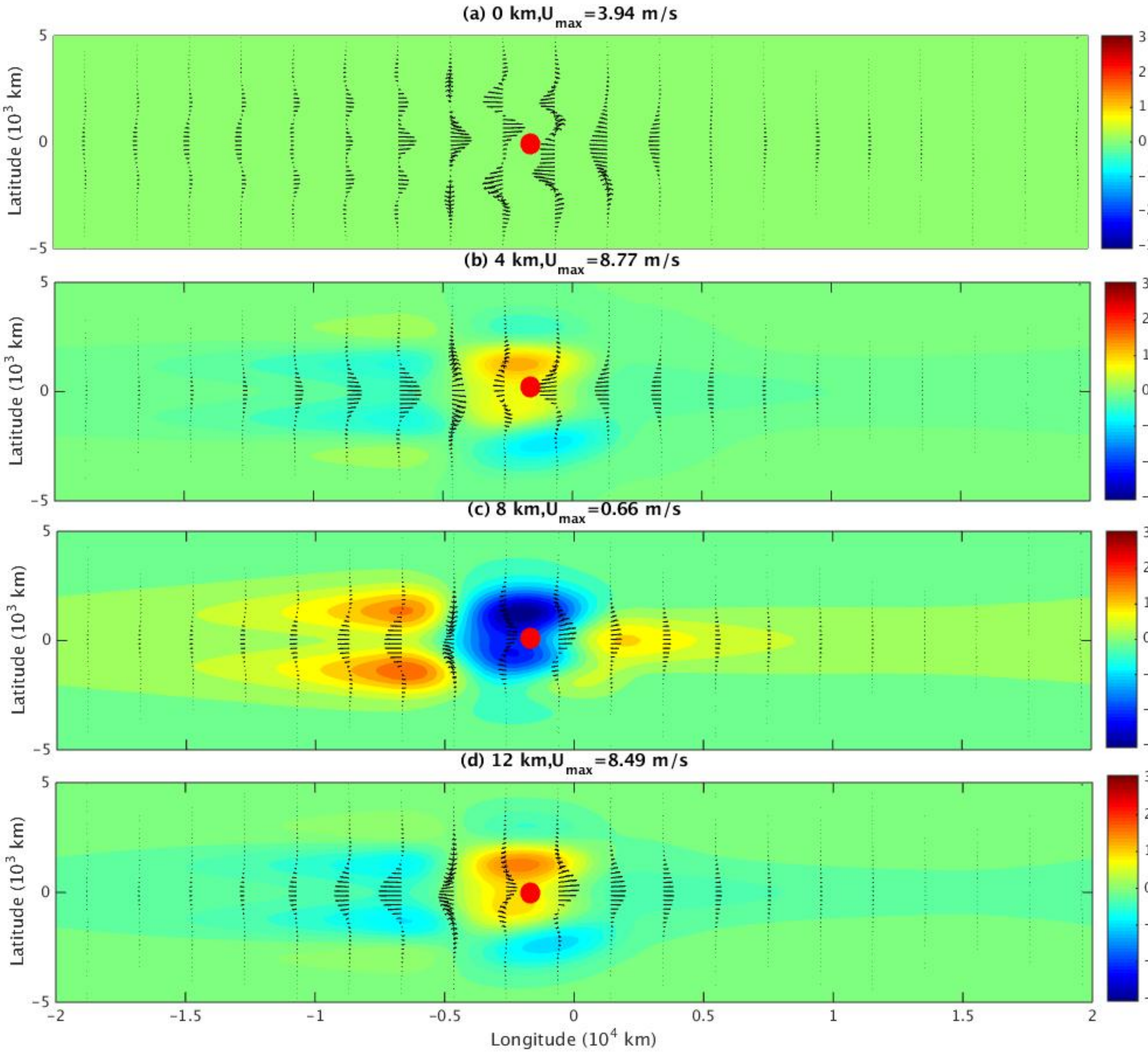

FIG. 17. The temperature anomalies associated with the equatorially symmetric MJO and the intraseasonal impact of the diurnal cycle at phase II. The color shows temperature anomalies, the flow field is shown by vectors. From top to bottom, these 4 panels show the heights at z=0 km, z=4 km, z=8 km, z=12 km. The unit of temperature anomaly is K. The red dot shows the center of the MJO convective activities.

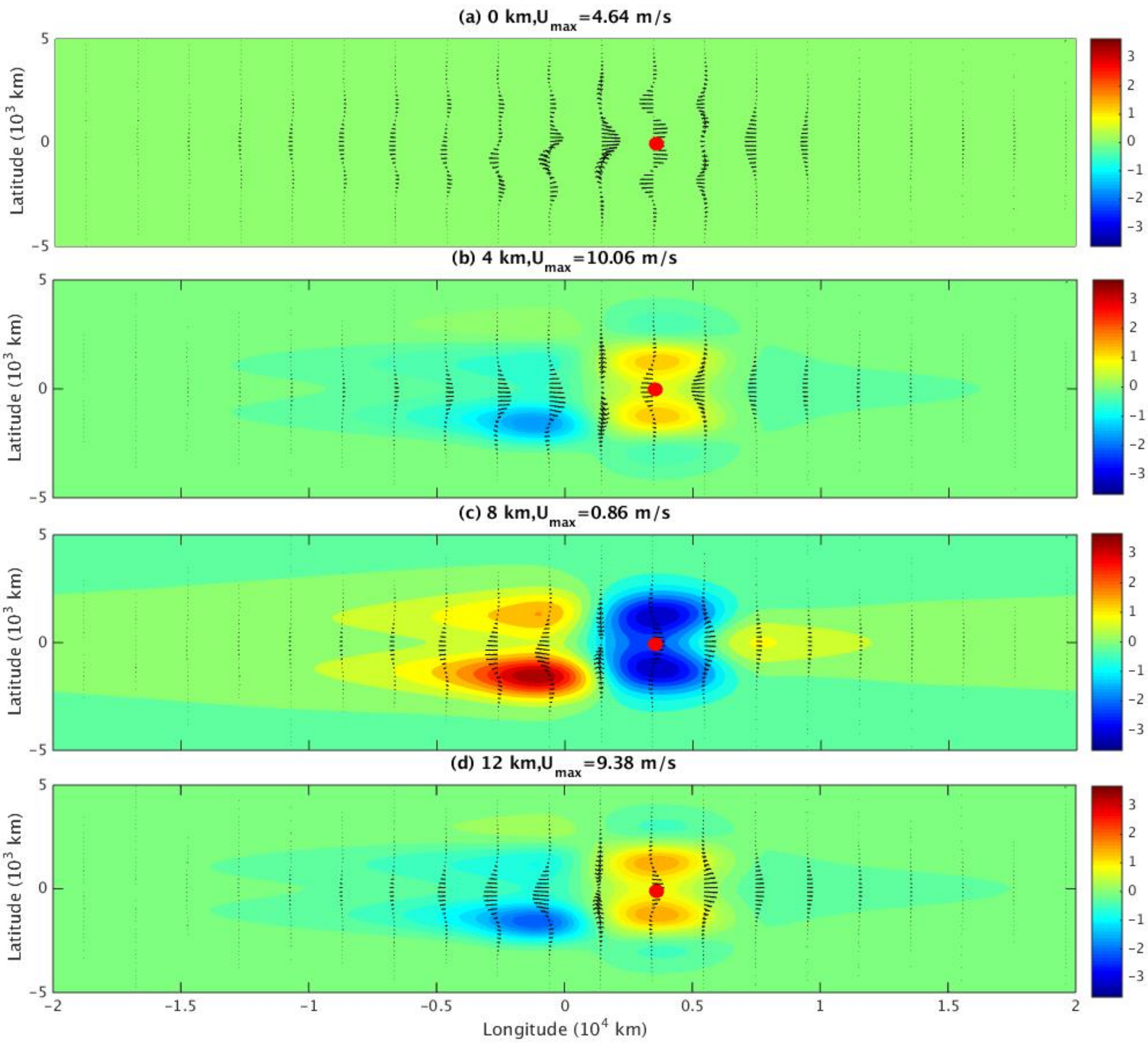

FIG. 18. The temperature anomalies associated with the equatorially symmetric MJO and the intraseasonal impact of the diurnal cycle at phase III. The color shows temperature anomalies, the flow field is shown by vectors. From top to bottom, these 4 panels show the heights at z=0 km, z=4 km, z=8 km, z=12 km. The unit of temperature anomaly is K. The red dot shows the center of the MJO convective activities.

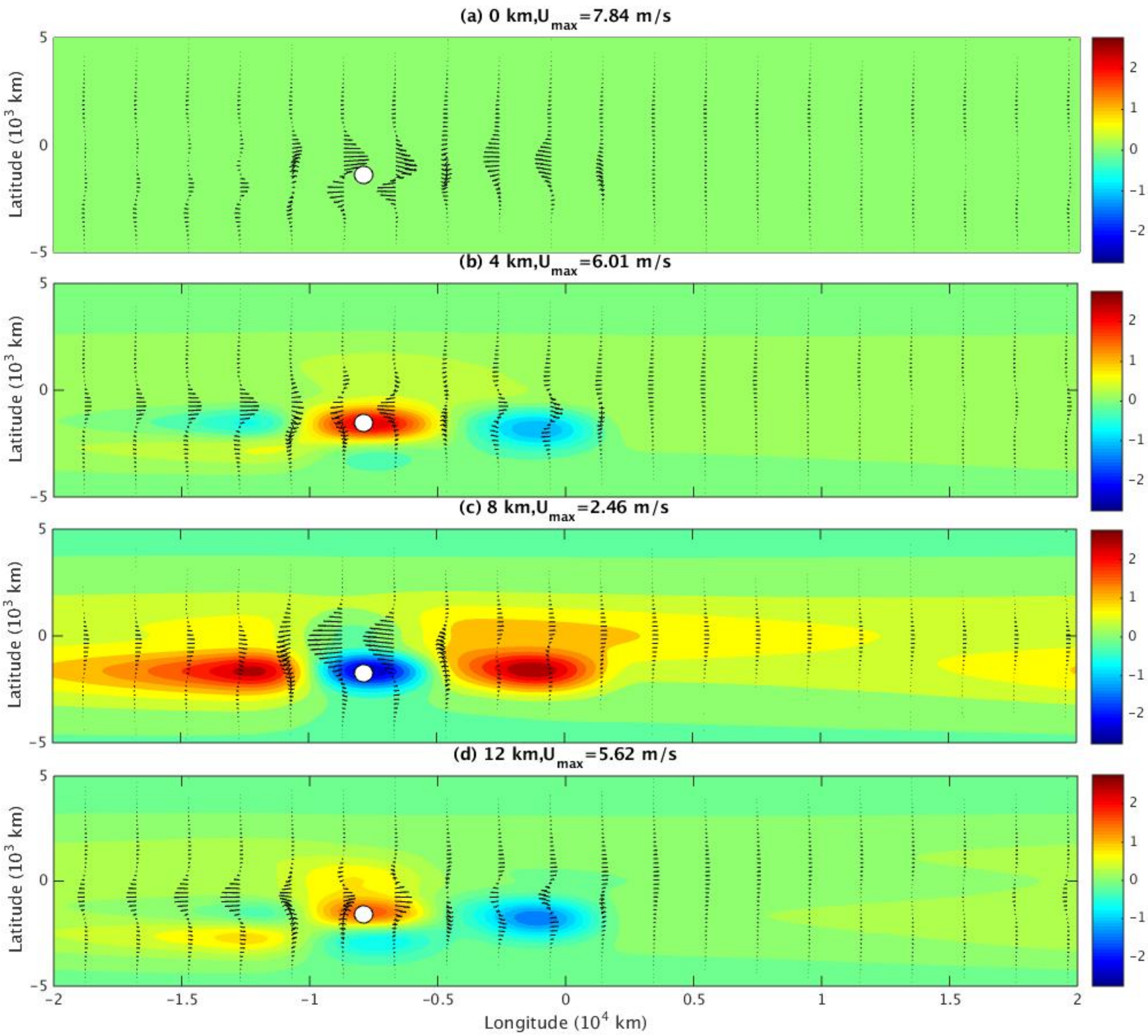

FIG. 19. The temperature anomaly under the intraseasonal impact of the diurnal cycle during the passage of the asymmetric MJO at Phase I. The panels shows flow vectors, red means positive temperature anomaly, and blue means negative temperature anomaly at heights (a) 0, (b) 4, (c) 8, (d) 12 km. The temperature anomaly is in units of K. The white dot shows the heating center.

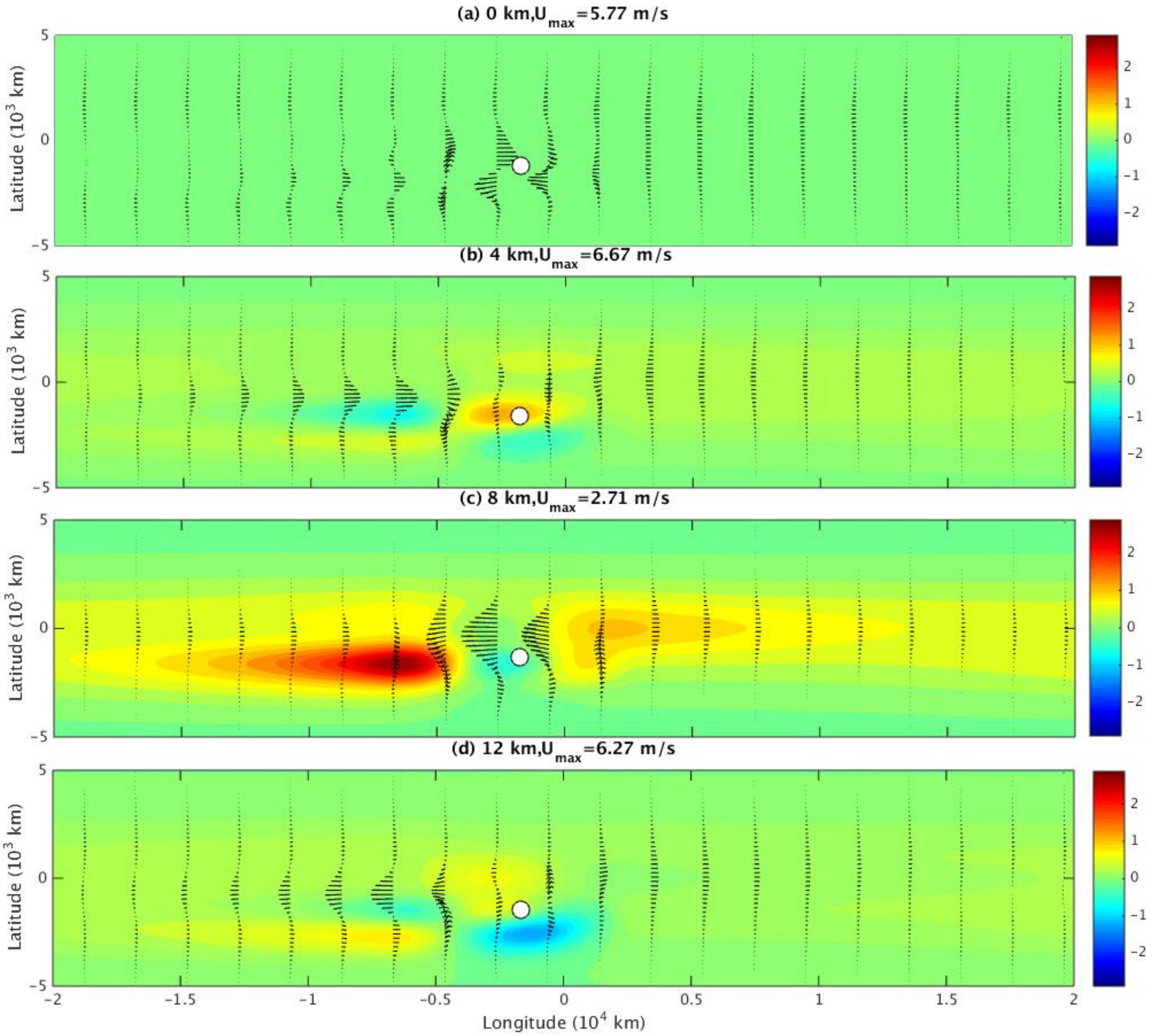

1032 FIG. 20. The temperature anomaly under the intraseasonal impact of the diurnal cycle during the passage of the asymmetric MJO at Phase II. The panels shows flow vectors, red means positive temperature anomaly, and blue means negative temperature anomaly at heights (a) 0, (b) 4, (c) 8, (d) 12 km. The temperature anomaly is in units of K. The white dot shows the heating center.

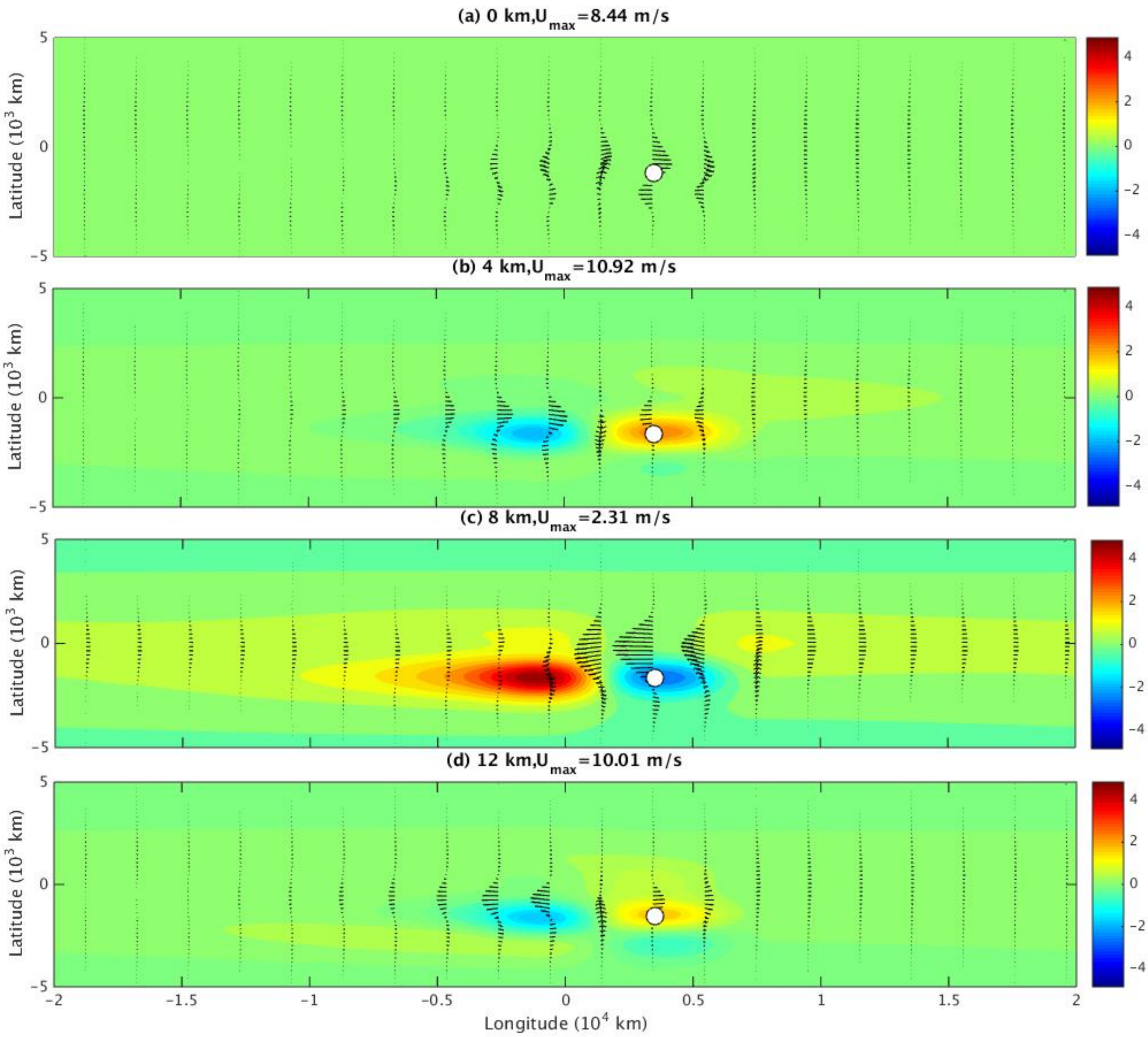

FIG. 21. The temperature anomaly under the intraseasonal impact of the diurnal cycle during the passage of the asymmetric MJO at Phase III. The panels shows flow vectors, red means positive temperature anomaly, and blue means negative temperature anomaly at heights (a) 0, (b) 4, (c) 8, (d) 12 km. The temperature anomaly is in units of K. The white dot shows the heating center.